Copy 6
RM E52E28

NACA RM E52E28

NACA

RESEARCH MEMORANDUM

PRELIMINARY INVESTIGATION OF FLOW FLUCTUATIONS DURING SURGE AND BLADE ROW STALL IN AXIAL-FLOW COMPRESSORS

By Merle C. Huppert

Lewis Flight Propulsion Laboratory
Cleveland, Ohio

NATIONAL ADVISORY COMMITTEE FOR AERONAUTICS

WASHINGTON
August 13, 1952

NATIONAL ADVISORY COMMITTEE FOR AERONAUTICS

RESEARCH MEMORANDUM

PRELIMINARY INVESTIGATION OF FLOW FLUCTUATIONS DURING SURGE AND BLADE ROW STALL IN AXIAL-FLOW COMPRESSORS

By Merle C. Huppert

SUMMARY

A preliminary investigation of the flow fluctuations of surge and blade row stall was conducted with three single-stage axial-flow compressors with hub-tip ratios of 0.9, 0.8, and 0.5 and a multistage axial-flow compressor.

Flow fluctuations of large amplitude associated with stall were detected in all compressors investigated. The fluctuations were caused by low flow regions affecting 25 to 40 percent of the annulus area and propagating in the direction of compressor rotation, but at a lower speed. Two apparently distinct types of propagating stall were detected. The first type consisted of a single stalled region with reversed flow which occurred following a sharp drop in compressor pressure ratio. The stalled region propagated in the direction of rotor rotation at approximately one-third compressor speed. The second type consisted of several equally spaced stalled regions associated with a progressive stall along the rotor blade span. The stalled regions propagated in the direction of rotor rotation at approximately 85 percent of rotor speed.

Mild audible surge was obtained with the single-stage compressors with hub-tip ratios of 0.9 and 0.8. No audible surge was detected with the 0.5 hub-tip ratio stage.

A severe audible surge was obtained with the multistage axial-flow compressor. The surge point was coincident with the sharp drop in pressure ratio due to stall.

INTRODUCTION

Compressor surge is generally considered to be the result of an instability of the flow process in the compressor and the system to which it is attached. The instability results in large flow and pressure fluctuations that may produce vibrations and audible sounds in the compressors and auxiliary system. The characteristic audible sounds produced as well as the fluctuations in pressure measuring instruments have

generally been used to detect the condition of surge in compressor performance evaluation.

Surge is an important problem in jet engine operation because of the limit it imposes on engine starting and acceleration. Inasmuch as surge is the low flow limit of the compressor, it may be encountered during engine acceleration if there is insufficient margin between the surge limit line of the compressor and the equilibrium operating line of the jet engine. In some engines, particularly those having high pressure ratios, the equilibrium operating line may cross the surge line at intermediate rotative speeds.

Observations of the characteristics of the pressure fluctuations within the compressor during surge (references 1 and 2) indicate that the frequency and amplitude of the pressure fluctuations are somewhat affected by the volume of the chamber between the compressor and its outlet throttle. In general, a decrease in volume resulted in a decrease in the amplitude of the pulsation and an increase in the frequency, but in no significant change of the weight flow at which surge occurred.

The conditions required for flow instability (surge) are studied theoretically in references 2 to 4. In reference 2, it is reported that, theoretically, surge is likely to occur when the slope of the compressor characteristic curve of pressure ratio against weight flow at a given rotational speed is positive, while the authors of reference 4 indicate that surge in multistage axial-flow compressors may occur when the slope is slightly negative. In general, a positive slope of the compressor characteristic curve is caused by stall of all or part of the blading in the compressor. The slope of the over-all compressor characteristic is approximately the average of the slope of the individual stages (see reference 5). Inasmuch as some of the stages may be stalled over a considerable part of the surge-free operating range of a compressor, stall is not a sufficient condition for surge, although stall generally exists in some part of the compressor at the surge point.

Recently it has been observed that blade row stall may produce rather large flow fluctuations. In reference 6 it is stated that stalling of the diffuser vanes of a centrifugal compressor may be nonuniform because of small differences between the vanes. These differences may cause one vane to stall before the others, giving rise to a reversed flow through that diffuser passage. This reversed flow will interfere with the flow in the adjacent vane (in the direction of the tangential velocity) and cause it to stall, and so on around the compressor. After the adjacent vane has stalled the originally stalled vane unstalls such that air flows in through part of the impeller eye and out through the rest of the eye. The stalled region rotates in the direction of impeller rotation, but more slowly. A similar phenomenon observed during stall

with an impulse axial-flow compressor rotor is reported in reference 7. The reversed flow region was detected by means of tufts on the rotor blades and annulus walls ahead of and behind the rotor. The reversed flow region occupied from 15 to 40 percent of the annulus area.

Reference 8 reports the results of a rather extensive hot-wire anemometer investigation on a centrifugal compressor consisting of an inducer and impeller discharging into a vaneless diffuser. Two distinct pulsating flow regions separated by stable regions were found, one initiated by impeller flow instability and the other, by inducer flow instability. Reference 2 reports three unstable regions separated by stable regions of flow. Only the most severe pulsations associated with a sharp drop in pressure ratio were audible. The type of stall phenomenon reported by references 6 and 7 was also detected in the inducer section of the compressor of reference 8; however, more than one stalled region was found to exist. At some operating conditions five distinct stalled regions were detected, and the stalled regions propagated in the direction of wheel rotation but more slowly, as was the case with the diffuser stalling reported in reference 6.

The phenomenon of self propagating or rotating stall is, in general, a different type of instability from that associated with surge. The various surge theories presented in the past (references 2 to 4) have considered the compressor as a simple one-dimensional device the flow through which becomes unstable when the pressure ratio has reached its maximum for a given speed. In reality the compressor blade rows consist of numerous diffusing passages operating in parallel. Self propagating or rotating stall is an instability associated with this parallel operation of blade passages, whereas surge is associated with the instability of the compressor operating in series with a receiver and a throttle.

Inasmuch as stall is, in general, a necessary condition for surge, the flow fluctuations of propagating stall are likely to be present in some part of the compressor prior to surge.

The significance of the self propagating or rotating regions of reversed flow is not completely understood at present. However, it is evident that large-scale fluctuations may occur in a compressor which is not surging audibly. Whether such large-scale inaudible fluctuations are detrimental to the compressor remains to be determined; however, they are a possible exciting force for blade vibrations.

In multistage axial-flow compressors, stall of any stage with local reverse flow may have a considerable effect on the preceding and the following stages. If the stalled region were to extend to other stages, the through flow would be concentrated in somewhat less than the full annulus area, thus increasing the axial velocity in these regions.

The purpose of this investigation at the NACA Lewis laboratory is the further study of the nature of the flow through single-stage and multistage axial-flow compressors when stall and surge are encountered. Surveys were made with hot-wire anemometers in three single-stage axial-flow compressors with hub-tip ratios of 0.9, 0.8, and 0.5. Surge in a 16-stage axial-flow compressor designed for a pressure ratio of 8.75 was investigated by the use of hot-wire anemometers and pressure transducers.

APPARATUS

Single-Stage Compressor Installations

A schematic diagram of a single-stage compressor setup is shown in figure 1. Air entered through the orifice tank and a motor-operated inlet throttle into a depression tank equipped with screens to provide a uniform distribution of air at the compressor inlet. Air was discharged from the compressor into a receiver connected to the altitude-exhaust system by two outlet pipes. The instrumentation used to obtain over-all performance was similar to that described in reference 9.

Three single-stage configurations each with a rotor tip diameter of 14 inches were used in this investigation: a typical exit stage of a multistage compressor with a hub-tip ratio of 0.9, a typical middle stage with a hub-tip ratio of 0.8, and a typical inlet stage with a hub-tip ratio of 0.5. All stages were designed for constant enthalpy and approximately symmetrical velocity diagrams at all radii except the 0.9 hub-tip ratio stage, which was straight bladed with a symmetrical velocity diagram at the pitch radius. The number of blades in each blade row of the compressor is listed in the following table:

Compressor hub-tip ratio	Number of guide vanes	Number of rotor blades	Number of stator blades
0.9	38	31	32
.8	40	44	24
.5	40	19	20

The vector diagrams for the three single-stage compressors are shown in figure 2. The diagrams for the 0.9 and 0.8 hub-tip ratio compressor are design diagrams, whereas the diagrams for the 0.5 hub-tip ratio compressor were computed from the test data at design speed and weight flow.

Multistage Compressor Installation

The compressor investigated was designed for a pressure ratio of 8.75 and a weight flow of 155 pounds per second with a rotor tip diameter of 33.5 inches. The over-all performance of the compressor and a description of the installation are given in reference 10.

Instruments for Detecting Flow Fluctuations

Hot-wire anemometers made of tungsten wire 0.0002 inch in diameter and 0.08 inch in effective length and oriented normal to the mean flow direction were used to measure and detect flow fluctuations. Constant wire-temperature operation was employed by the methods described in reference 11. The amplifier incorporates negative feedback such that the anemometer resistance (and consequently temperature) is maintained constant. The instantaneous voltage drop across the wire necessary to maintain its resistance constant was amplified and recorded either on an oscillograph or photographically from a cathode ray oscilloscope. The time-average anemometer current was measured by an ammeter.

The method of converting the voltage fluctuation across the anemometer to fluctuations in mass flow rate ρV used in interpreting the data is presented in appendix A. An audio-frequency oscillator was used in conjunction with the cathode ray oscilloscope to determine the frequency of the fluctuations.

Pressure fluctuations were measured with strain-gage-type pressure transducers used in conjunction with a strain analyzer and a recording oscillograph. The pressure transducers were used to measure the fluctuations in stagnation pressure.

RESULTS

The results consist largely of oscillograms of hot-wire anemometer and pressure transducer output. An explanation of propagating stall and a method of determing the number of stalled regions and their direction of rotation are included in appendix B. This information is required for the interpretation of the test results.

Single-Stage Compressor with Hub-Tip Ratio of 0.9

Hot-wire anemometers were installed at each of two stations in the compressor: at the pitch radius at station 0 about 1/2 inch upstream of the inlet guide vanes, and at the pitch radius at station 3 about 1/2 inch downstream of the stator (see fig. 1).

The compressor performance map is shown in figure 3. The regions where large amplitude fluctuations were first indicated by the anemometers as the air flow was reduced are shown by the shaded areas. A typical oscillogram showing these fluctuations is presented in figure 4. (The symbols used herein are defined in appendix C.) The top trace was obtained from the anemometer installed at station 0 upstream of the inlet guide vanes and the bottom trace, from the anemometer installed at station 3 downstream of the stator blades. The signal from the anemometer at station 3 was filtered so that flow fluctuations with a frequency greater than 1000 cps, largely blade wakes, are not shown on the oscillogram. The filter caused a 180° phase shift in the signal so that a reduction in flow is indicated by a downward deflection of the lower trace from station 3 and by an upward deflection of the top trace from station 0. The amplitude of the fluctuations in mass flow rate ρV divided by the mean value $\Delta\rho V/\overline{\rho V} = 1.2$, as determined by the method of appendix A. This is a rough average of the value from several oscillograms and is given only to indicate the amplitude of the fluctuations.

The installation of two anemometers at station 0 (one anemometer was kept in a fixed position and the other was located at each of several angular positions from the fixed anemometer) showed, by the methods presented in appendix B, that there was one region of low flow and that it was revolving about the axis of rotation of the compressor at a rotative speed less than that of the compressor but in the same direction.

The following table summarizes the hot-wire data obtained at three compressor speeds:

Compressor rotative speed $N/\sqrt{\theta}$ (rps)	Frequency with which stall passed anemometer f (cps)	Number of low flow regions in annulus λ	$\frac{h}{N/\sqrt{\theta}}$
167	51	1	0.306
200	61	1	.305
233	71	1	.305

These data indicate that the stall propagates around the axis of this compressor at about 30 percent of the compressor speed and is evidently much the same as the pressure-rise stall discussed in reference 7. Reverse flow was indicated by the oscillograms obtained with a weight flow somewhat lower than that at which the oscillogram shown in figure 4 was obtained.

Audible surge was not encountered in the speed range for which overall performance was obtained (fig. 3). However, audible surge with a frequency of from 10 to 15 cps was obtained at a speed $N/\sqrt{\theta} = 267$. At this speed the flow fluctuations of propagating stall when first encountered were intermittent, appearing and disappearing during the flow fluctuations of the surge.

Single-Stage Compressor with Hub-Tip Ratio of 0.8

In order to investigate the stall and surge characteristics of this stage, two hot-wire anemometers were installed between the rotor and the stator (station 2, fig. 1) in radial traversing mechanisms. Provisions were made for locating the anemometers at each of several angular positions.

The performance characteristics of this compressor at equivalent rotative speeds $N/\sqrt{\theta}$ of 162 rps and 207 rps are shown in figure 5. Stall was first encountered at the rotor tip and was indicated by an increase in the size of the blade wakes. An oscillogram of initial stall of the rotor tip and an oscillogram of the normal tip wake are shown in figure 6. A slight further reduction in weight flow resulted in a whistling sound at the point marked A on the performance curve shown in figure 5. Oscillograms obtained at six radial positions at point A (fig. 5) with two anemometers separated by angle $\alpha = 60^\circ$ are shown in figure 7. The frequency of the fluctuations was 1120 cps, and eight stalled regions were indicated by use of the methods of appendix B. The stalled regions were propagating in the direction of compressor rotation. The amplitude of the fluctuations at the blade tip is somewhat larger than that of those at the blade root. As the weight flow was reduced to that at point B (fig. 5), the stall pattern remained the same but the amplitude of the fluctuations at the root was increased, with no appreciable change at the tip.

A sharp drop in pressure ratio occurred with a slight reduction in weight flow from point B as indicated in figure 5, and the oscillogram taken at point C appears as shown in figure 8. The stall frequency f was 59 cps and one stall region was indicated by the method of appendix B. The amplitude of the fluctuations $\Delta\rho V/\overline{\rho V}$ is approximately 1.3, about the same as with the single-stage compressor with hub-tip ratio of 0.9 (fig. 4).

A hysteresis loop was noted in that the sharp rise in pressure ratio did not occur until the weight flow was increased to a value (point D, fig. 5) larger than that at which the sharp drop in pressure ratio occurred.

Surge was not encountered at an equivalent compressor speed of 162 rps. The only flow fluctuations were due to the propagating stall regions.

At a compressor equivalent rotative speed $N/\sqrt{\theta} = 207$ the initial tip stall occurred at point E of figure 5. At a slightly reduced weight flow (indicated in fig. 5) a mild audible surge was obtained, and the higher frequency flow fluctuations of stall appeared to be intermittent on the oscilloscope screen. In order to measure the amplitude of the low frequency surge fluctuation the output of one of the two anemometers located at the rotor pitch section $\left(\alpha = 41\frac{1}{4}^{\circ}\right)$ was filtered to pass only those fluctuations of fewer than 100 cps and amplified with a d-c amplifier. The output of the other anemometer was filtered to pass all fluctuations of fewer than 12,000 cps and was amplified with an a-c amplifier. Motion pictures were taken of the oscilloscope screen during the surging condition. The fluctuations during a single surge cycle are shown in figure 9. The lower trace is from the anemometer whose output was filtered to pass fluctuation with a frequency of less than 100 cps, and the top trace is from the anemometer filtered to pass frequencies up to 12,000 cps. The amplitude of the surge flow fluctuations $\Delta\rho V/\overline{\rho V}$ varied somewhat from cycle to cycle but on the average was approximately 0.10. The surge frequency varied from 10 to 15 cps. The amplitude of the fluctuations of stall varies in phase with the mass flow rate variation due to surge. The maximum amplitude of the stall fluctuation $\Delta\rho V/\overline{\rho V}$ is approximately 0.6.

As the weight flow was reduced to point G the surging stopped, leaving only the flow fluctuations of propagating stall. Figure 10 shows oscillograms obtained at 6 radial positions at this weight flow (point G, fig. 5). The flow fluctuations are much the same in amplitude as those obtained at an equivalent compressor speed of 162 rps shown in figure 7. There were eight stalled regions propagating in the direction of compressor rotation but at a lower speed. The frequency of the fluctuations was, however, somewhat higher - 1420 cps as compared with 1120 cps at an equivalent rotative speed of 162 rps.

As the weight flow was further reduced the number of stalled regions remained the same, but the amplitude of the fluctuations at the rotor root increased. At point H of figure 5 a sharp drop in pressure ratio occurred. The oscillogram obtained at point I is shown in figure 11. These are the flow fluctuations of a single revolving stall with a frequency of 77 cps and the amplitude of the fluctuations was approximately the same at all radii.

In order to investigate the manner in which the eight stalled regions changed abruptly at point H to one stall at point I (fig. 5), motion pictures were taken of the oscilloscope while the compressor

outlet throttle was being closed. Figure 12 shows the oscillogram obtained at the time of the sharp drop in pressure ratio. The higher frequency fluctuations are the same as those shown in figure 10 and the large fluctuations at the right of the figure indicate a single large stalled region the same as that shown in figure 11, but the time scale is increased in figure 12 so that the wave form of the large stalled region can be seen better. Inasmuch as the hot-wire anemometers used indicated magnitude of the mass flow rate only and not direction, a reversed flow region would be indicated as a second peak near the center of the low flow region, as shown in figure 12.

The following table summarizes the data taken on the single-stage compressor with a hub-tip ratio of 0.8:

Compressor rotative speed $N/\sqrt{\theta}$ (rps)	Frequency with which stall passed anemometer f (cps)	Number of stalled regions λ	$\frac{h}{N/\sqrt{\theta}}$	Point on compressor performance map (fig. 5)
162	1120	8	0.89	A
162	59	1	.36	C
207	1420	8	.85	G
207	77	1	.37	I

Single-Stage Compressor with Hub-Tip Ratio of 0.5

In order to investigate the stall and surge characteristics of this stage, two hot-wire anemometers were installed between the rotor and the stator (station 2, fig. 1). The anemometers were located with angle $\alpha = 105^{\circ}$ each in a radial traversing mechanism.

Hot-wire anemometer data were obtained at only one compressor speed $N/\sqrt{\theta} = 225$ and the compressor performance characteristics at that speed are shown in figure 13. The compressor weight flow at which tip stall was first encountered is indicated by point A in figure 13. The hot-wire anemometer traces obtained at three radial positions with the compressor operating at point B are shown in figure 14. The frequency of the stall was approximately 1200 cps. Although the fluctuations at the outer radial positions are quite large, the fluctuations at $R = 0.714$ are small. The data taken were insufficient to determine the number of stalled regions. Although the weight flow was reduced to very low values, there was no value at which the pressure ratio dropped sharply and the stall pattern changed abruptly as occurred with the compressor with a hub-tip ratio of 0.8. Furthermore, surge was not detected at any weight flow.

Multistage Axial-Flow Compressor

The surge and stall studies of the multistage axial-flow compressor were confined to low rotative speeds. With pressure transducers at the compressor inlet stage and discharge annulus and two hot-wire anemometers in the seventh stage stator, the compressor was taken into surge at an equivalent rotative speed of 51 rps.

Figure 15 shows the stagnation pressure fluctuations at the compressor inlet and discharge during surge. During each surge pulse the inlet stagnation pressure increased approximately $8\frac{1}{2}$ percent ($\Delta P/P_0 = +0.085$), and the discharge pressure decreased approximately 17 percent ($\Delta P/P_3 = -0.17$). The surge frequency varied from 1 to 2 cps. The pressure fluctuations at the compressor inlet occur practically simultaneously with the fluctuations at the compressor discharge.

In order to show the small, higher frequency fluctuations superimposed on the larger surge fluctuations, the time scale is increased considerably in figure 15(b). These smaller fluctuations are believed to be due to propagating stall.

The hot-wire anemometer traces shown in figure 16 also show the presence of propagating stall in the seventh stage. These data indicate a flow fluctuation $\Delta\rho V/\overline{\rho V} = \pm 0.3$ attributable to the surge pulse. The amplitude of the flow fluctuation of the largest amplitude propagating stall was $\Delta\rho V/\overline{\rho V} = 1.2$.

These data indicate that during surge propagating stall extends throughout the compressor; however, the data obtained were insufficient to determine the number of stalled regions.

Inasmuch as the amplitude of surge increased considerably with rotative speed for this compressor, an effort was made to reduce the amplitude of surge and increase its frequency. To accomplish this the volume of the receiver chamber between the compressor and the outlet throttle was reduced to approximately one-tenth its original value. Fixed-area orifices were used as a throttle, and the compressor was operated with the orifices choked. The operating line with the fixed-area orifice intersected the surge line at an equivalent rotative speed $N/\sqrt{\theta} = 53$. The oscillogram of compressor discharge stagnation pressure against time as the surge line was encountered is shown in figure 17.

Audible surge was not obtained, but small nonperiodic fluctuations in compressor discharge stagnation pressure were noted prior to the sharp drop in pressure ratio which occurred as the previously established surge line was crossed. The stagnation pressure at the compressor discharge

decreased about 17 percent ($\Delta P/P_3 = -0.17$). After the sharp drop in pressure ratio a propagating stall with a frequency of 58 cps and an amplitude $\Delta P/P_3 = -0.05$ is indicated (fig. 17). The pressure fluctuation with a frequency of about 12 cps, which occurred following the sharp drop in pressure ratio, may be due to mild surge, although it was inaudible. The data taken were insufficient to positively identify this condition as surge. A hot-wire anemometer installed in the first-stage stator also indicated the propagating stall. These data indicate that the propagating stall probably extended through the entire 16 stages of the compressor, just as was indicated in the surge data of figures 15 and 16.

The sharp drop in pressure at the surge line obtained with the low volume receiver is evidently analogous to the similar phenomenon observed in the single-stage compressor with a hub-tip ratio of 0.8.

Some indication of large amplitude fluctuations of propagating stall in the inlet stages at weight flows somewhat larger than the flow for surge was obtained at compressor speeds between 30 and 40 percent of design speed.

No detailed measurements have been made to determine which stages initiate the propagating stall or how far the phenomenon extends from the initiating stage. However, the analysis of reference 5 indicates that, in general, the inlet stages will be stalled at low compressor speeds.

DISCUSSION OF RESULTS

Propagating Stall

Large amplitude flow fluctuations of propagating stall were observed in each of the three single-stage compressors and the multistage compressor. These data and the information included in references 5 to 7 leave little doubt that pressure-rise stall of all blades of a compressor rotor is unstable. Propagating stall is the result of this instability. Theory for predicting the number of stalled regions and their propagating rate is not yet available.

The propagating stall obtained with the three single-stage compressors may be separated into two types:

1. Single stall region, low frequency propagating stall. This type of stall propagates at approximately one-third rotor speed in the direction of rotor rotation; the amplitude of the flow fluctuations $\Delta\rho V/\overline{\rho V}$ is about 1.2 in the compressors investigated. Reversed flow was indicated

in the middle of the stalled regions (figs. 11 and 12) in some cases. Inasmuch as a sharp drop in compressor pressure ratio occurs simultaneously with the beginning of this stall, it may be considered as the low flow limit of the efficient operating range of the stage. The flow fluctuation amplitude is approximately the same at all radii with this type of stall.

2. Multiple stall region, high frequency propagating stall. This type of stall propagates at approximately 85 percent of rotor speed in the direction of rotor rotation (figs. 7 and 10). This propagating stall was initiated by rotor tip stall and the amplitude of the flow fluctuations associated with it varies with radius. The largest fluctuations ($\Delta\rho V/\overline{\rho V} = 0.7$) occur at the rotor tip. This type of propagating stall is associated with progressive stall along the rotor blade length and consequently with a gradual decrease in compressor pressure ratio as weight flow is reduced rather than with the sharp decrease associated with stall of type 1.

The data from the single-stage compressor with hub-tip ratio of 0.9 indicate propagating stall of type 1. However, data were not obtained with anemometers at station 2 (fig. 1) between the rotor and the stator.

The single-stage compressor with hub-tip ratio of 0.8 exhibited propagating stall of both types 1 and 2. Stall of type 2 was started by stall at the rotor tip and persisted until type 1 occurred with its attendant sharp drop in pressure ratio (see fig. 5).

The single-stage compressor with hub-tip ratio of 0.5 exhibited only type 2 stall. Although the data obtained were insufficient to determine the number of stalled regions, the amplitude and frequency of the flow fluctuations suggest type 2 stall. Even though the weight flow through the compressor was reduced to very low values a sharp drop in pressure ratio did not occur. This effect may be similar to that in the inducer section of a centrifugal pump, as explained in reference 12, where the stalled region at the inducer tip is thought of as a ring eddy. The eddy increases in size as the weight flow is reduced, thus keeping the axial velocity at the blade root sufficiently high to prevent complete stall of the blading.

The data obtained from the multistage compressor were not sufficiently complete to determine the number of stalled regions under any condition. However, the amplitude of large fluctuations during surge suggests type 1 stall. The data obtained with the low volume receiver, which apparently eliminated severe surge, also indicate type 1 stall. The sharp drop in pressure ratio, whether accompanied by surge or not, indicates the low flow limit of the efficient operating range of the compressor.

Propagating stall was confined to the front stages of the compressor at weight flows larger than the flow for surge at low compressor speeds. Although the extent to which propagating stall in any stage of a multistage compressor affects the performance of preceding and succeeding stages is unknown, it seems likely that type 1 stall may have a pronounced effect because the through flow is concentrated in somewhat less than the full annulus area.

The flow fluctuations of propagating stall may be an excitation force for blade vibrations. Inasmuch as the flow fluctuation frequency increases linearly with rotative speed, resonant vibration could be excited at particular compressor speeds.

Surge

The surge obtained with the single-stage compressors with hub-tip ratios of 0.8 and 0.9 may be described as mild audible pulsations; the flow fluctuation of surge $\Delta\rho V/\overline{\rho V}$ with the 0.8 hub-tip ratio compressor (see figs. 5 and 9) was about 0.10 at frequencies of from 10 to 15 cps. The amplitude of the pressure fluctuations during surge was not measured but was probably small.

The surge obtained with the multistage compressor at $N/\sqrt{\theta} = 51$ with the large volume receiver was a large amplitude or severe audible surge. Flow fluctuations $\Delta\rho V/\overline{\rho V}$ of ± 0.3 and stagnation pressure fluctuations at the compressor discharge $\Delta P/P_3$ of about -0.17 were found at frequencies of from 1 to 2 cps (see figs. 15 and 16).

Large surge amplitude did not occur with the small volume receiver between the compressor and outlet throttle. A sharp drop in compressor discharge stagnation pressure occurred as the surge line was crossed at $N/\sqrt{\theta} = 53$. The amplitude of the pressure drop was about 17 percent of the compressor discharge pressure, or about the same as the drop in pressure during surge with the large receiver volume.

The data of figures 15 and 16 indicate that the mass flow rate as indicated by the hot-wire anemometer in the seventh-stage stator is a maximum when the compressor discharge pressure is a minimum and that the mass flow rate decreases as the compressor discharge pressure increases at the end of the surge pulse.

SUMMARY OF RESULTS

A preliminary investigation of the flow fluctuation of blade row stall and compressor surge was conducted with three single-stage axial-flow compressors with hub-tip ratios of 0.9, 0.8, and 0.5 and a multistage axial-flow compressor.

Flow fluctuations of large amplitude associated with stall were detected in all compressors investigated. The fluctuations were caused by low flow regions affecting 25 to 40 percent of the annulus area propagating in the direction of compressor rotation, but at a lower speed. Two apparently distinct types of propagating stall were detected. The first type consisted of a single stalled region with reversed flow which occurred following a sharp drop in compressor pressure ratio. The stalled region propagated in the direction of rotor rotation at approximately one-third compressor speed. The second type consisted of eight equally spaced stalled regions associated with a progressive stall along the rotor blade span. The stalled regions propagated in the direction of rotor rotation at approximately 85 percent of rotor speed.

Mild audible surge was obtained with the single-stage compressors with hub-tip ratios of 0.9 and 0.8. No audible surge was detected with the 0.5 hub-tip ratio stage.

A severe audible surge was obtained with the multistage axial-flow compressor. The surge point was coincident with the sharp drop in pressure ratio due to stall.

Lewis Flight Propulsion Laboratory
National Advisory Committee for Aeronautics
Cleveland, Ohio

[redacted]

APPENDIX A

METHOD OF DETERMINING FLUCTUATIONS IN ρV FROM OSCILLOGRAMS

The oscillogram of the hot-wire anemometer output is a measure of the voltage drop across the anemometer necessary to maintain it at a fixed resistance and consequently constant temperature. The time-average value of the anemometer current is proportional to the time-average value of voltage drop across the anemometer.

$$\bar{e} = \bar{i}\Omega \tag{A1}$$

The voltage drop e across the anemometer is related to the flow rate ρV past the anemometer by the heat-transfer characteristics of a heated wire in an air stream. Reference 14 indicates that the heat-transfer characteristics of hot-wire anemometers can be correlated satisfactorily by the following formula (King's law):

$$i^2\Omega = (C_1 + g(M)C_2\sqrt{\rho V})(T_w - T_e) \tag{A2}$$

The factor $g(M)$ is a function of Mach number, and both C_1 and C_2 are determined by calibration. Solving (A2) for ρV results in the following expression:

$$\rho V = \left[\frac{i^2\Omega}{C_2 g(M)(T_w - T_e)} - \frac{C_1}{C_2 g(M)}\right]^2 \tag{A3}$$

By use of the relation $e = i\Omega$,

$$\rho V = \left[\frac{e^2}{\Omega(T_w - T_e)g(M)C_2} - \frac{C_1}{g(M)C_2}\right]^2 \tag{A4}$$

If the effect of Mach number on $g(M)$ and possible variation in T_e during a fluctuation in ρV are neglected,

$$\rho V = g(e) \tag{A5}$$

Fluctuation in ρV will cause variations in e about some time-average value $\bar{e}$; then

$$\rho V = g(e) = g(\bar{e} + \Delta e) \tag{A6}$$

Inasmuch as primary interest is in the magnitude of the ρV fluctuations compared with the average value, it will be convenient to express the ρV fluctuations in terms of the voltage fluctuation across the anemometers as measured from the oscillograms. Defining

$$\overline{\rho V} \equiv \left[\frac{\bar{e}^2}{\Omega(T_w - T_e)C_2 g(M)} - \frac{C_1}{g(M)C_2}\right]^2 = g(\bar{e}) \tag{A7}$$

and expanding (A6) in a Taylor series give

$$g(e) = g(\bar{e}) + \Delta e\, g'(\bar{e}) + \frac{(\Delta e)^2 g''(\bar{e})}{2!} + \frac{(\Delta e)^3 g'''(\bar{e})}{3!} + \frac{(\Delta e)^4 g''''(\bar{e})}{4!} \tag{A8}$$

Using

$$g(\bar{e}) = \left(\frac{\bar{e}^2}{A} - B\right)^2 \tag{A9}$$

where

$$A = \Omega(T_w - T_e)C_2 g(M)$$

$$B = \frac{C_1}{C_2 g(M)}$$

(A and B are assumed constant during fluctuation in ρV.)

$$g'(e) = \frac{4\bar{e}}{A}\left[f(\bar{e})\right]^{\frac{1}{2}}$$

$$g''(\bar{e}) = \frac{4\left[f(\bar{e})\right]^{\frac{1}{2}}}{A} + \frac{8\bar{e}^2}{A^2} \tag{A10}$$

$$g'''(\bar{e}) = \frac{24\bar{e}}{A^2}$$

$$g''''(\bar{e}) = \frac{24}{A^2}$$

When (A10) is substituted in (A8),

$$g(e) = g(\bar{e}) + \frac{\bar{e}^4}{A^2}\left[4\left(\frac{\Delta e}{\bar{e}}\right)^2 + 4\left(\frac{\Delta e}{\bar{e}}\right)^3 + \left(\frac{\Delta e}{\bar{e}}\right)^4\right] + \frac{\left[g(\bar{e})\right]^{\frac{1}{2}}\bar{e}^2}{A}\left(4\frac{\Delta e}{\bar{e}} + 2\frac{\Delta e^2}{\bar{e}}\right) \tag{A11}$$

results. Rearranging (A11) and dividing both sides by $g(\bar{e})$ give

$$\frac{g(\bar{e}) - g(e)}{g(\bar{e})} = \frac{\bar{e}^4}{A^2 g(\bar{e})}\left[4\left(\frac{\Delta e}{\bar{e}}\right)^2 + 4\left(\frac{\Delta e}{\bar{e}}\right)^3 + \left(\frac{\Delta e}{\bar{e}}\right)^4\right] +$$

$$\frac{\bar{e}^2}{A\left[g(\bar{e})\right]^{\frac{1}{2}}}\left[4\frac{\Delta e}{\bar{e}} + 2\left(\frac{\Delta e}{\bar{e}}\right)^2\right] \tag{A12}$$

From (A6) and (A7),

$$\frac{g(e) - g(\bar{e})}{g(\bar{e})} = \frac{\rho V - \overline{\rho V}}{\overline{\rho V}} = \frac{\Delta \rho V}{\overline{\rho V}} \tag{A13}$$

The factor

$$\frac{\bar{e}^2}{A\left[g(\bar{e})\right]^{\frac{1}{2}}} = \frac{\bar{e}^2}{A\left(\frac{\bar{e}^2}{A} - B\right)} = \frac{\bar{e}^2}{\bar{e}^2 - AB} = \frac{1}{1 - \frac{AB}{\bar{e}^2}} \tag{A14}$$

From (A9)

$$\frac{AB}{\bar{e}^2} = \frac{C_1 \Omega (T_w - T_e)}{\bar{e}^2}$$

but

$$C_1 = \frac{e_0^2}{\Omega (T_w - T_a)}$$

When $\rho V = 0$, $e = e_0$ so

$$\frac{AB}{\bar{e}^2} = \left(\frac{e_0}{\bar{e}}\right)^2$$

and

$$\frac{\bar{e}^2}{A\left[g(\bar{e})\right]^{\frac{1}{2}}} = \frac{1}{1 - \left(\frac{e_0}{\bar{e}}\right)^2} \tag{A15}$$

Substituting (A15) and (A13) in (A12) yields

$$\frac{\Delta\rho V}{\overline{\rho V}} = \left[\frac{1}{1 - \left(\frac{e_0}{\bar{e}}\right)^2}\right]\left\{4\frac{\Delta e}{\bar{e}} + 2\left(\frac{\Delta e}{\bar{e}}\right)^2 + \left[\frac{1}{1 - \left(\frac{e_0}{\bar{e}}\right)^2}\right]\left[4\left(\frac{\Delta e}{\bar{e}}\right)^2 + 4\left(\frac{\Delta e}{\bar{e}}\right)^3 + \left(\frac{\Delta e}{\bar{e}}\right)^4\right]\right\} \tag{A16}$$

A plot of $\Delta\rho V/\overline{\rho V}$ against $\Delta e/\bar{e}$ for various values of $e_0/\bar{e}$ is presented in figure 22. The mass flow rate ρV is zero when

$$\frac{\Delta e}{\bar{e}} = \frac{e_0 - \bar{e}}{\bar{e}} = \frac{e_0}{\bar{e}} - 1$$

APPENDIX B

EXPLANATION OF PROPAGATING STALL AND METHOD OF DETERMINING NUMBER OF STALLED REGIONS

Explanation of Propagating Stall

An explanation of propagating stall is given in references 6 to 8. A similar explanation is included here for completeness.

A two-dimensional cascade of compressor blades (diffusing) is considered stalled when the maximum turning is obtained or when the maximum value of static pressure rise divided by inlet velocity head $\Delta p/q$ is reached, as indicated in figure 18. (See reference 13.) An explanation of the instability of uniform stall of all blades in the cascade may be made considering the two-dimensional cascade characteristics. Suppose a compressor rotor is operating such that some blade section along the span is at a stalled condition (pressure-rise stall) and that the stall is uniform from blade to blade in the rotor. A local reduction in velocity at some position will cause the local flow angle β relative to the rotor to exceed the stall angle and, as indicated in figure 18, the blades subjected to the higher flow angle are incapable of supporting the pressure rise of the rest of the blades. The flow in the affected blade passages will consequently break down completely and the flow will be greatly reduced and possibly reversed in direction. Because of this reduction or reversal in flow, incoming air will be spilled to adjacent blade passages, as shown in figure 19. This spillage will subject the blades on one side of the affected passages to higher flow angles and the blades on the other side to lower flow angles as shown. In this manner the low flow region propagates around the annulus as indicated in figure 20. This new flow pattern with propagating stall is evidently stable, but the through flow is concentrated in somewhat less than the full annulus area.

Method of Determining Number of Stalled Regions by Use of Two Anemomemters Displaced Angularly in Compressor Annulus

In order to derive the expression necessary to determine the number of stalled regions by use of two anemometers displaced angularly in the plane of instrumentation (fig. 21(a)), it will be convenient to assume that the number of stalls and their direction of rotation are known.

The stalled region passes each anemometer station f times per second, and

$$f = h\lambda \tag{B1}$$

The output signals of the two anemometers displaced angularly α degrees appear on the oscilloscope as shown in figure 21(b). If the stalled regions are rotating clockwise as indicated in figure 21(a), stall will pass each anemometer every $1/f$ seconds, and a given stall will pass anemometer 1 first and pass anemometer 2, $\frac{\alpha}{360h}$ seconds later. Inasmuch as the stalls are quite similar, one stall cannot be distinguished from another, so $\frac{\alpha}{360h}$ cannot, in general, be determined from a single oscillogram. The phase shift, that is, the time x, can be read directly from the oscillogram. For the example shown,

$$x = \frac{\alpha}{360h} - \frac{1}{f} \tag{B2}$$

Then the ratio $\frac{x}{1/f} = \frac{\alpha f}{360h} - 1 = y$

Since

$$\nu = \frac{360}{\lambda} = \frac{h360}{f}$$

then

$$y = \frac{\alpha}{\nu} - 1 \tag{B3}$$

If there had been twice as many stalled regions,

$$x = \frac{\alpha}{360h} - \frac{2}{f}$$

$$y = \frac{\alpha}{\nu} - 2$$

Then, in general, with the stalls rotating in the direction shown in figure 21(a),

$$x = \frac{\alpha}{360h} - \frac{n}{f}$$

and

$$y = \frac{\alpha}{\nu} - n \tag{B4}$$

where n is the number of stalls enclosed in angle α and, consequently, an integer. The value of y then varies with α/ν as shown in figure 21(c). When equation (B4) is differentiated with respect to α,

$$\frac{dy}{d\alpha} = \frac{1}{\nu} = \frac{\lambda^+}{360} \tag{B5}$$

is obtained provided α/ν is not an integer, in which case the derivative does not exist in the usual sense because y is discontinuous at these points.

If the stalls had been rotating in the direction opposite (counterclockwise) to that indicated in figure 21(a), a stall would have passed anemometer 2 before passing anemometer 1. For counterclockwise rotation the oscillograms would appear as shown in figure 21(d). In this case,

$$x = \frac{2}{f} - \frac{\alpha}{360h}$$

and

$$y = 2 - \frac{\alpha}{\nu} \tag{B6}$$

If there had been twice as many stalls,

$$y = 3 - \frac{\alpha}{\nu}$$

and, in general,

$$y = n + 1 - \frac{\alpha}{\nu} \tag{B7}$$

A plot of y against α/ν is shown in figure 21(e) where n is, as before (equation (B4)), the number of stalls enclosed in angle α and, consequently, an integer. Differentiation of (B7) with respect to α gives

$$\frac{dy}{d\alpha} = -\frac{1}{\nu} = -\frac{\lambda^-}{360} \tag{B8}$$

provided α/ν is not an integer, in which case the derivative (B8) does not exist.

In order to determine the number of stalls λ in any given case, two anemometers are needed with provision for varying the angle α. If one of the anemometers is on a movable mount such that α may be varied continuously, λ can be determined unambiguously from equation (B5) or (B8).

[redacted]

When the anemometers are located in fixed positions such that α is changed by steps, the number of stalls n included in each value of α must be considered. From equation (B4) and

$$\nu = \frac{360}{\lambda}$$

there is obtained

$$y = \frac{\alpha\lambda^+}{360} - n \tag{B9}$$

or

$$\lambda^+ = (y + n)\frac{360}{\alpha}$$

for stall rotating clockwise. From (B7),

$$y = n + 1 - \frac{\alpha\lambda^-}{360}$$

or

$$\lambda^- = (n + 1 - y)\frac{360}{\alpha} \tag{B10}$$

for counterclockwise rotation of the stalled regions.

For various values of α, y is determined from the oscillograms; then λ may be computed for values of $n = 0,1,2,3,\ldots k$ by use of equations (B9) and (B10), and tabulated as shown in the accompanying table. Unless y is measured quite accurately λ may not be an integer; however, the nearest integer should be tabulated.

α	y	n	λ^+	λ^-
α_1	y_1	0	$0^{\lambda+}{}_1$	$0^{\lambda-}{}_1$
		1	$1^{\lambda+}{}_1$	$1^{\lambda-}{}_1$
		2	$2^{\lambda+}{}_1$	$2^{\lambda-}{}_1$
		3	$3^{\lambda+}{}_1$	$3^{\lambda-}{}_1$
		k	$k^{\lambda+}{}_1$	$k^{\lambda-}{}_1$
α_2	y_2	0	$0^{\lambda+}{}_2$	$0^{\lambda-}{}_2$
		1	$1^{\lambda+}{}_2$	$1^{\lambda-}{}_2$
		2	$2^{\lambda+}{}_2$	$2^{\lambda-}{}_2$
		3	$3^{\lambda+}{}_2$	$3^{\lambda-}{}_2$
		k	$k^{\lambda+}{}_2$	$k^{\lambda-}{}_2$
α_i	y_i	0	$0^{\lambda+}{}_i$	$0^{\lambda-}{}_i$
		1	$1^{\lambda+}{}_i$	$1^{\lambda-}{}_i$
		2	$2^{\lambda+}{}_i$	$2^{\lambda-}{}_i$
		3	$3^{\lambda+}{}_i$	$3^{\lambda-}{}_i$
		k	$k^{\lambda+}{}_i$	$k^{N-}{}_i$

The correct value of the number of stalls λ and their direction or rotation will appear for every value of anemometer spacing α and the corresponding value of y measured from the oscillogram. If the rotation is clockwise the correct value of λ will recur under the column λ^+, and if the rotation is counterclockwise the correct value of λ will recur in the column λ^-. If more than one value of λ recurrs, additional values of α must be tried to determine λ.

APPENDIX C

SYMBOLS

The following symbols are used in this report:

A	parameter, $\Omega(T_w - T_e)C_2 g(M)$
B	parameter, $C_1/C_2 g(M)$
C_1 and C_2	constants in equation for heat-transfer characteristics of hot-wire anemometer (see equation (A2))
e	voltage drop across hot-wire anemometer, volts
e_0	voltage drop across hot-wire anemometer with zero flow, volts
f	frequency with which disturbance passes hot-wire anemometer or pressure transducer, cps
g( )	indicates functional relation with quantity in parentheses
h	rotative speed of a propagating stall region, rps
i	current through hot-wire anemometer, amp
k,n	integers (see appendix B)
N	compressor rotative speed, rps
P	stagnation pressure, lb/sq ft
p	static pressure, lb/sq ft
q	$\frac{1}{2}\rho V^2$, lb/sq ft
R	ratio of radius to tip radius
T	temperature, $^{\circ}R$
U	rotor blade speed, ft/sec
V	velocity, ft/sec
W	velocity relative to rotor, ft/sec

w	weight flow, lb/sec
X	V_θ/U_t
x	time between appearance of a flow fluctuation on oscillogram from one of two anemometers and appearance of a flow fluctuation on other anemometer (see fig. 20), sec
Y	V_z/U_t
y	xf
α	angular displacement between two hot-wire anemometers, deg
β	angle between velocity and axial direction, deg
δ	compressor inlet stagnation pressure divided by standard pressure, $P_1/2116$
θ	compressor inlet stagnation temperature divided by standard temperature, $T_1/518.6$
λ	number of propagating stall regions in annulus
ν	angular displacement between two propagating stall regions, deg
ρ	density, slugs/cu ft
$\overline{\rho V}$	mass flow rate corresponding to time-average anemometer current, slugs/(sq ft)(sec) (see equation (A7))
Ω	resistance of hot-wire anemometer, ohms

Subscripts:

e	used as subscript on T to indicate effective gas temperature (see appendix A)
i	used to associate value of α and possible corresponding values of λ (see appendix B)
t	rotor tip
w	hot-wire anemometer
z	axial component
θ	tangential component

0	station at compressor inlet (fig. 1)
1	station between inlet guide vanes and rotor (fig. 1)
2	station between rotor and stator of single-stage compressors (fig. 1)
3	station at compressor discharge (fig. 1)

Subprescript:

0,1,...k	indicates value of n used in determining λ (see appendix B)

Superscripts:

+	indicates clockwise rotation of propagating stall
-	indicates counterclockwise rotation of propagating stall
'	(prime) indicates differentiation
$\overline{\ }$	(bar) indicates time-average value

REFERENCES

1. Brooke, G. V.: Surging in Centrifugal Supercharger. R.&M. No. 1503, British A.R.C. 1932.

2. Bullock, Robert O., Wilcox, Ward W., and Moses, Jason J.: Experimental and Theoretical Studies of Surging in Continuous-Flow Compressors. NACA Rep. 861, 1946. (Supersedes NACA TN 1213.)

3. Bullock, R. O., and Finger, H. B.: Surging in Centrifugal and Axial-Flow Compressors. Preprint No. 605, presented at SAE Nat. Aero. Meeting (New York), April 16-19, 1951.

4. Pearson, H., and Bower, T.: Surging in Axial Compressors. Aero. Quarterly, vol. 1, pt. III, Nov. 1949. (Pub. by Roy. Aero. Soc. (London).)

5. Finger, Harold B., and Dugan, James F., Jr.: Analysis of Stage Matching and Off-Design Performance of Multistage Axial-Flow Compressors. NACA RM E52D07, 1952.

6. Adams, H. T.: Elements of Internal Combustion Turbine Theory. Cambridge at the Univ. Press (London), 1949, p. 52.

7. Schulze, Wallace M., Erwin, John R., and Westphal, Willard R.: Investigation of an Impulse Axial-Flow Compressor Rotor over a Range of Blade Angles. NACA RM L50F27a, 1950.

[redacted]

8. Grant, Howard P.: Hot Wire Measurements of Stall Propagation and Pulsating Flow in an Axial Flow Inducer-Centrifugal Impeller System. Pratt and Whitney Res. Rep. No. 133, June 1951.

9. Burtt, Jack R.: Investigation of Performance of Typical Inlet Stage of Multistage Axial-Flow Compressor. NACA RM E9E13, 1949.

10. Medeiros, Arthur A., Guentert, Donald C., and Hatch, James E.: Performance of J35-A-23 Compressor. I - Over-All Performance Characteristic at Equivalent Speeds from 20 to 100 Percent of Design. NACA RM E50J17, 1951.

11. Ossofsky, Eli: Constant Temperature Operation of the Hot-Wire Anemometer at High Frequency. The Rev. of Sci. Instr., vol. 19, no. 12, Dec. 1948.

12. Spannhake, Wilhelm: Centrifugal Pumps, Turbines, and Propellers. The Technology Press, M.I.T. (Cambridge), Mass. 1934, pp. 247-249.

13. Herrig, L. Joseph, Emery, James C., and Erwin, John R.: Systematic Two-Dimensional Cascade Tests of NACA 65-Series Compressor Blades at Low Speeds. NACA RM L51G31, 1951.

14. Lowell, Herman H.: Design and Applications of Hot-Wire Anemometers for Steady-State Measurements at Transonic and Supersonic Airspeeds. NACA TN 2117, 1950.

[redacted]

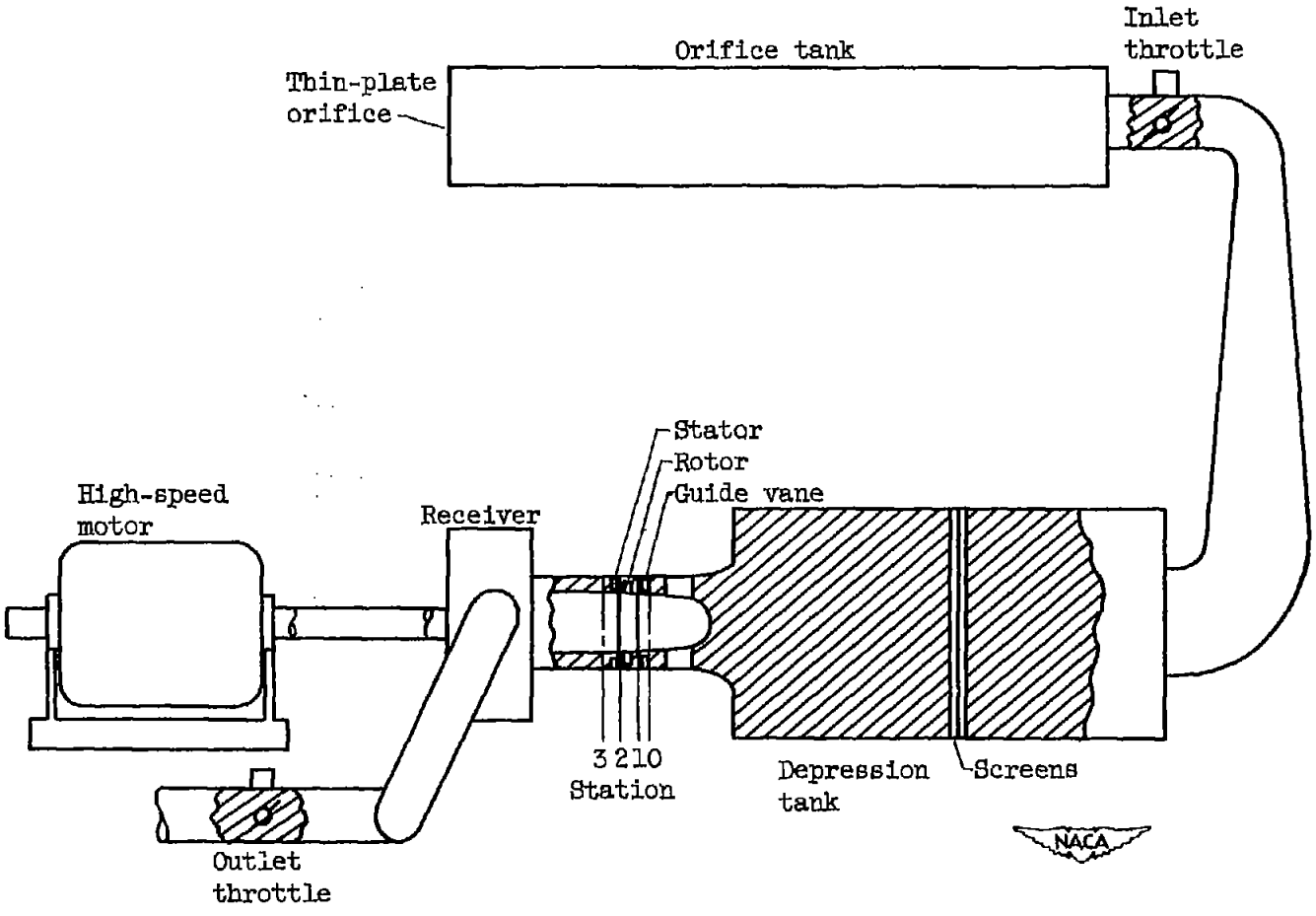

Figure 1. - Schematic diagram of compressor installation.

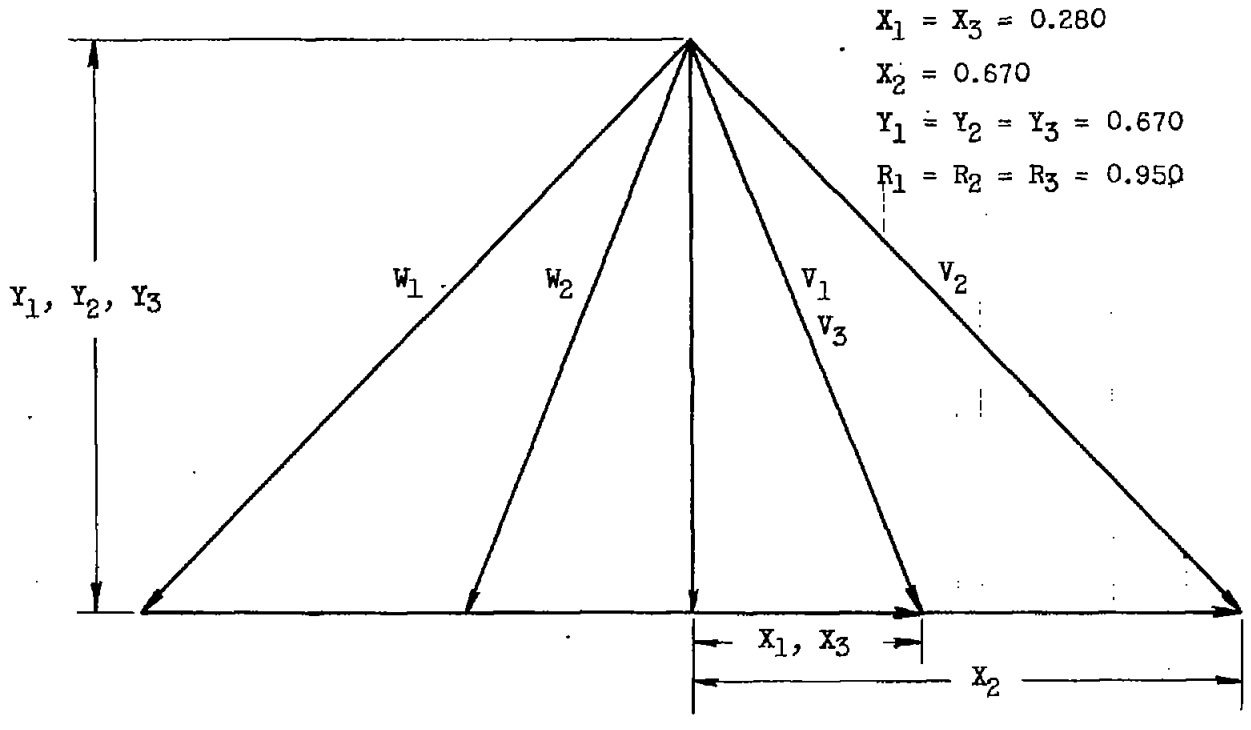

(a) 0.9 hub-tip ratio stage.

Figure 2. - Vector velocity diagrams for single-stage axial-flow compressors.

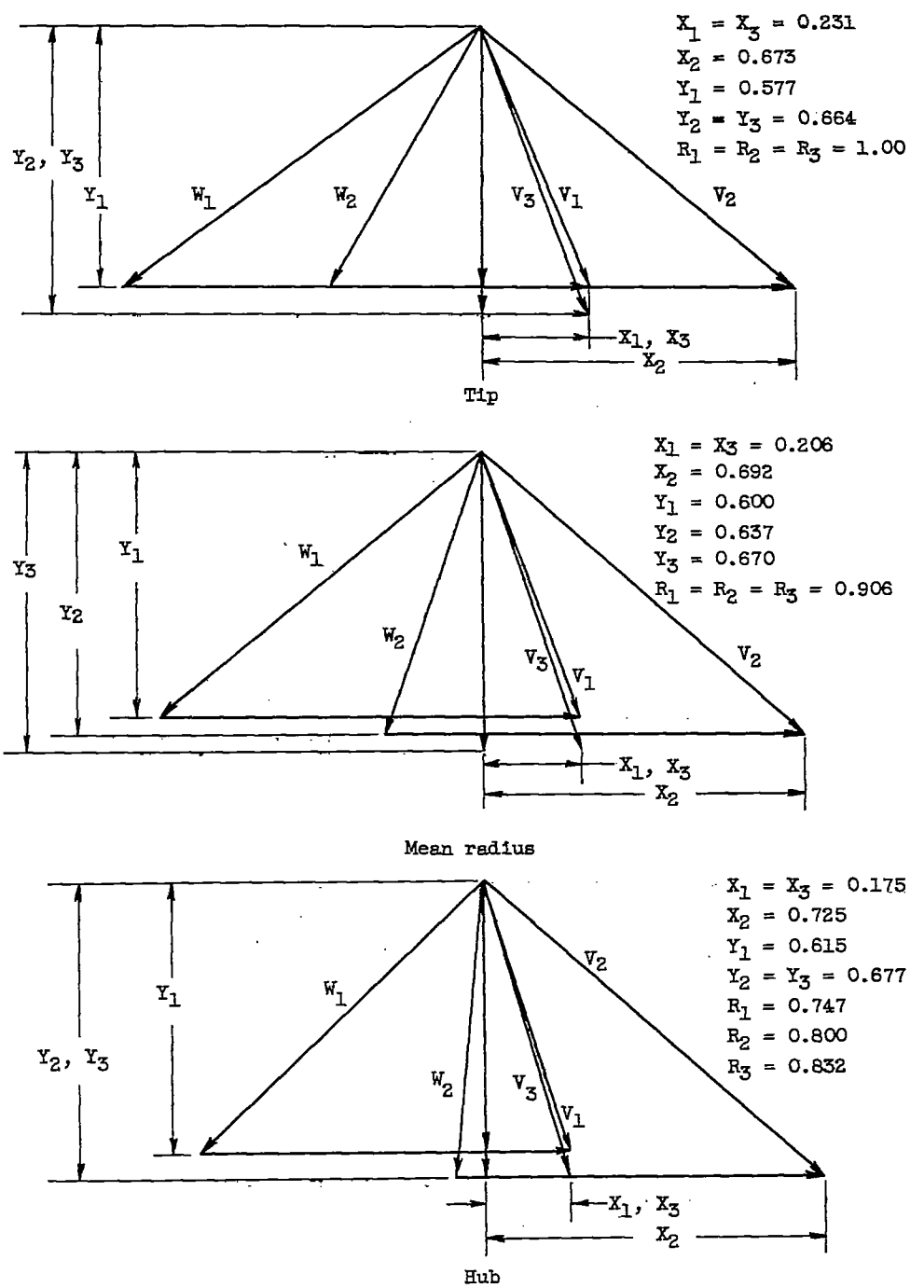

(b) 0.8 hub-tip ratio stage.

Figure 2. - Continued. Vector velocity diagrams for single-stage axial-flow compressors.

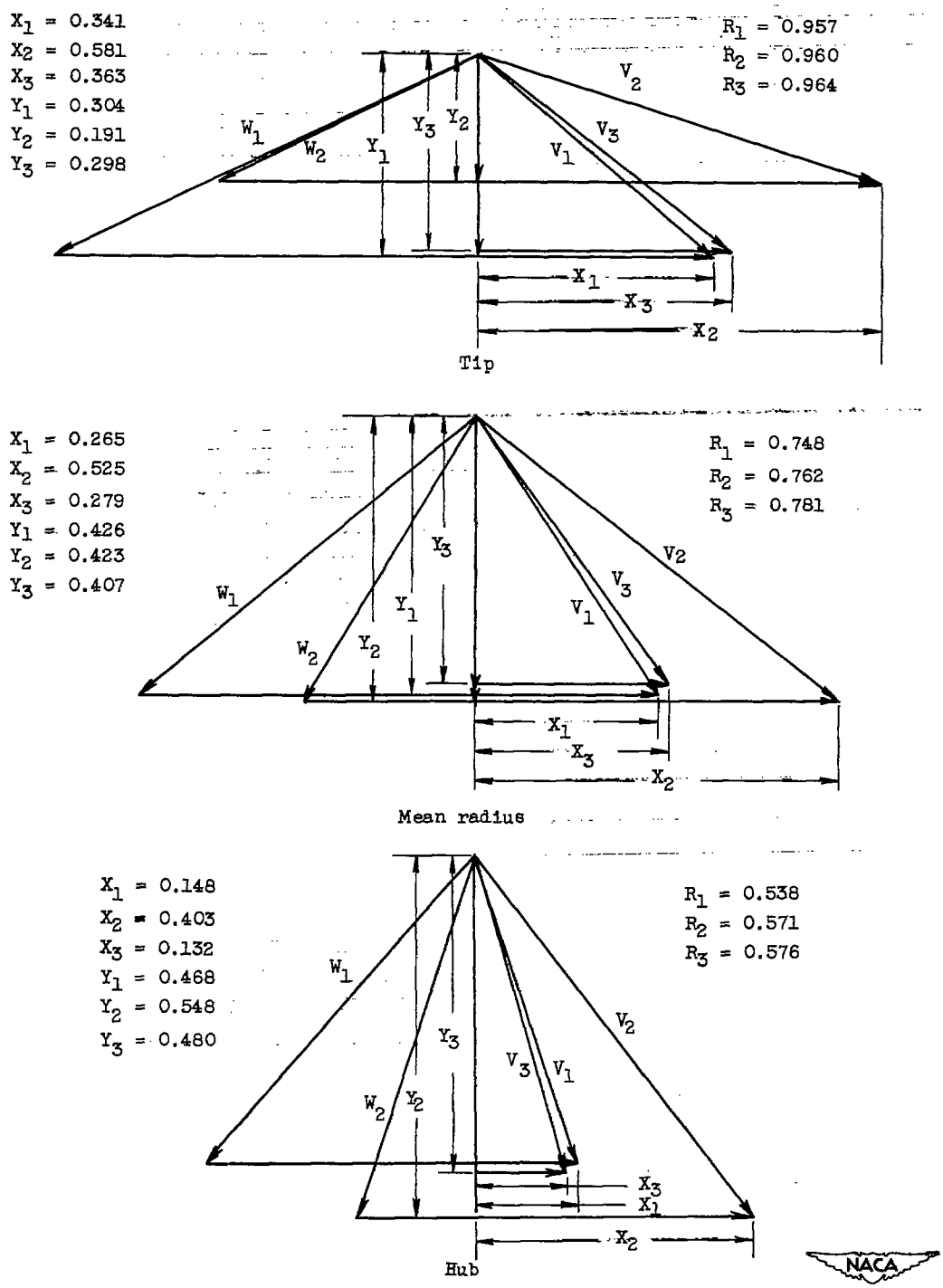

(c) 0.5 hub-tip ratio stage.

Figure 2. - Concluded. Vector velocity diagrams for single-stage axial-flow compressors.

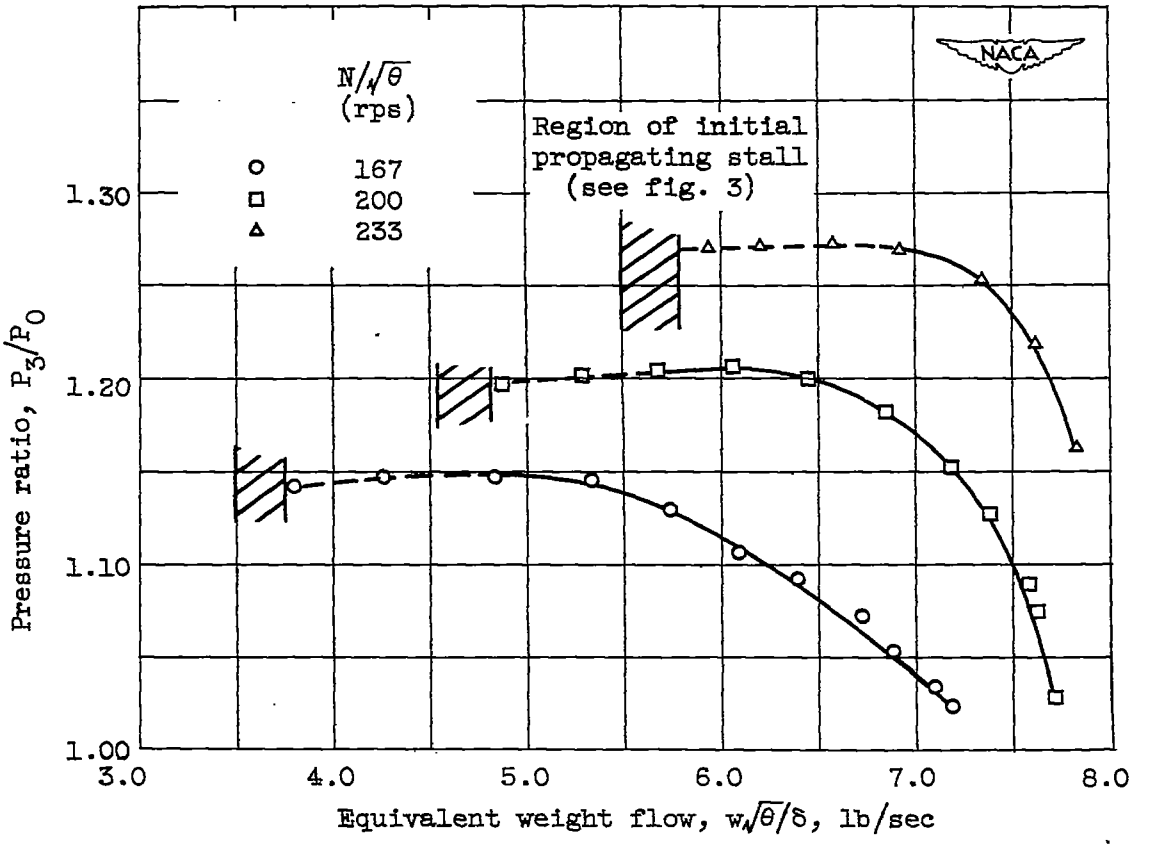

Figure 3. - Over-all performance of single-stage compressor with hub-tip ratio of 0.9.

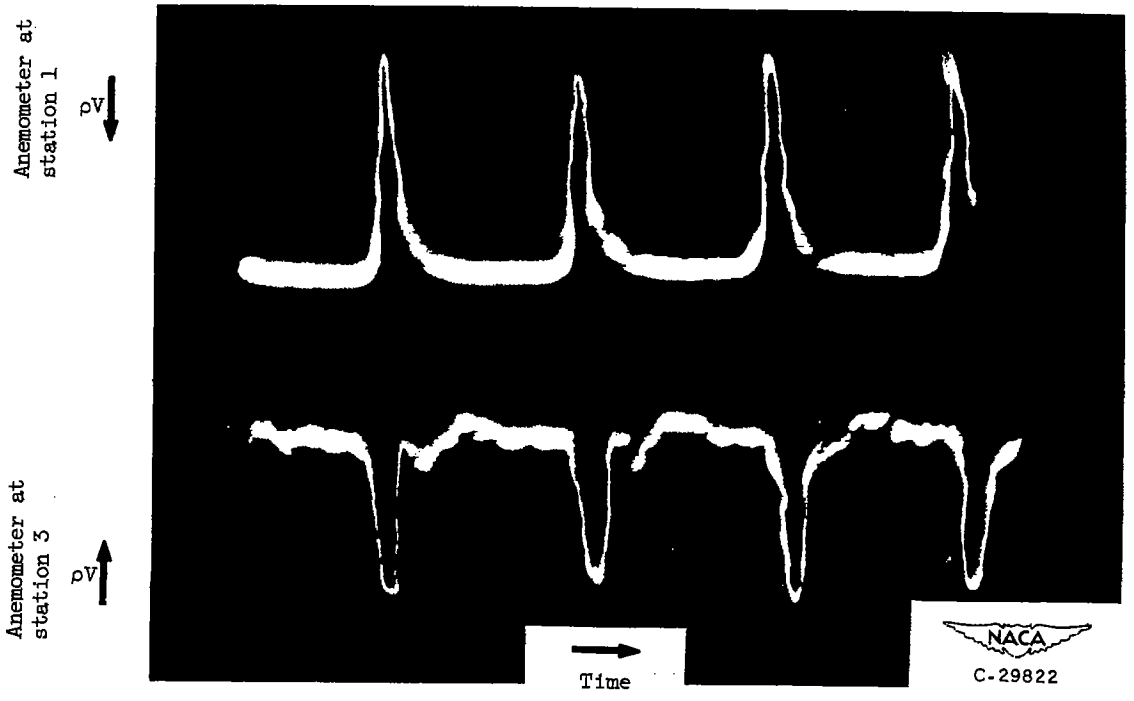

Figure 4. - Typical oscillogram obtained from hot-wire anemometer with rotating stall in single-stage compressor with hub-tip ratio of 0.9. $\Delta\rho V/\overline{\rho V} = 1.2$; f depends on rotative speed.

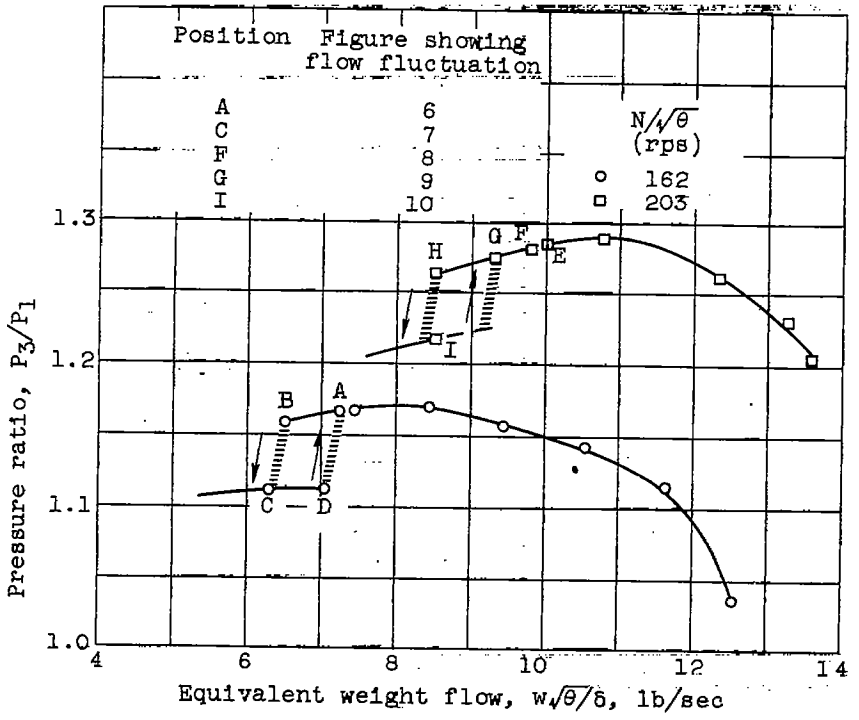

Figure 5. - Over-all performance of single-stage compressor with hub-tip ratio of 0.8.

(a) Blade wake at initial tip stall. $\Delta\rho V/\overline{\rho V} = 0.3$.

(b) Normal blade wake. $\Delta\rho V/\overline{\rho V} = 0.1$.

NACA
C-29793

Figure 6. - Comparison of blade wake at rotor tip at initial stall with normal wake for single-stage compressor with hub-tip ratio of 0.8. R = 0.98; f = 7130 cps; $N/\sqrt{\theta} = 162$.

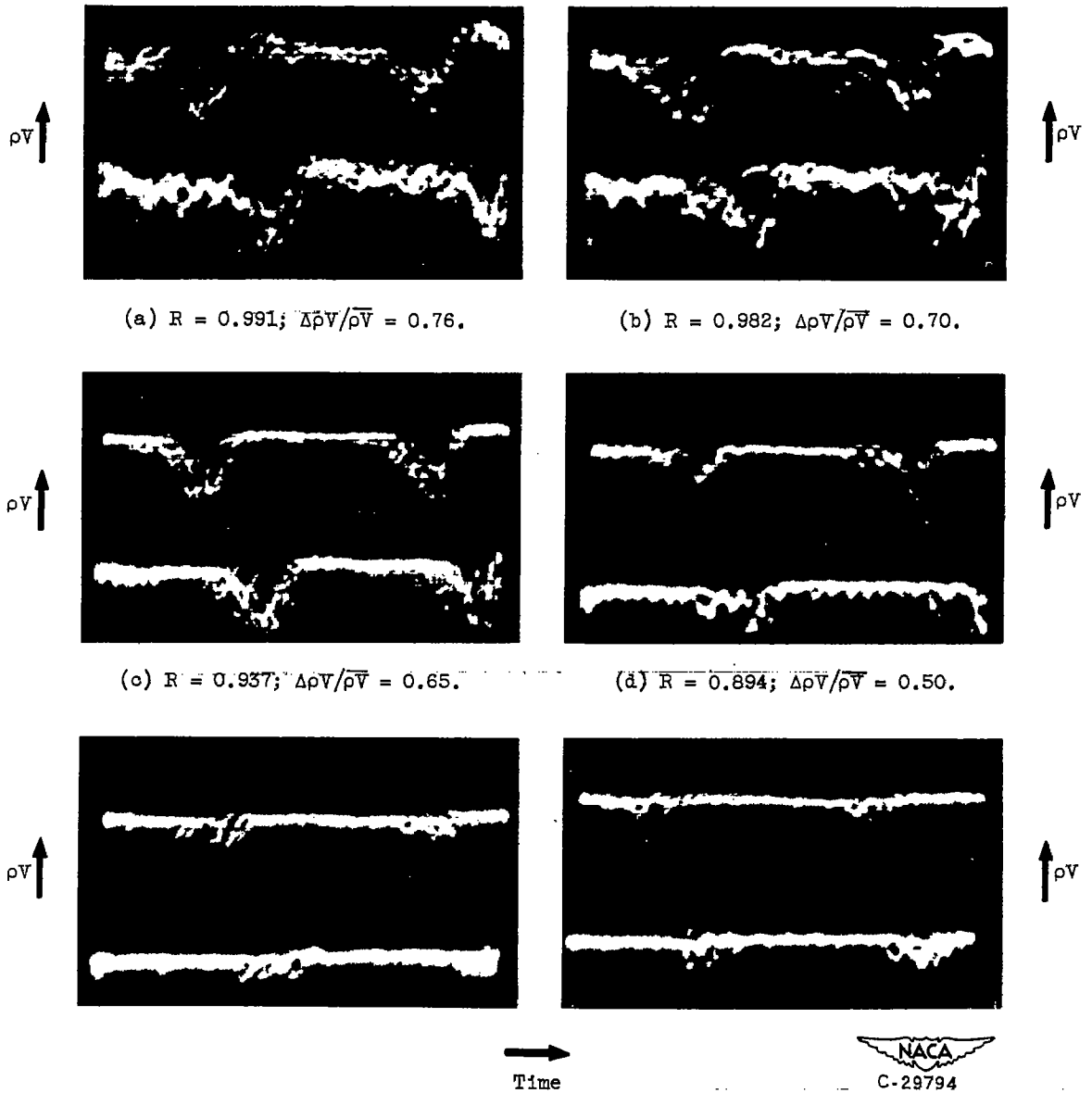

(a) R = 0.991; $\Delta\rho V/\overline{\rho V}$ = 0.76.

(b) R = 0.982; $\Delta\rho V/\overline{\rho V}$ = 0.70.

(c) R = 0.937; $\Delta\rho V/\overline{\rho V}$ = 0.65.

(d) R = 0.894; $\Delta\rho V/\overline{\rho V}$ = 0.50.

(e) R = 0.851; $\Delta\rho V/\overline{\rho V}$ = 0.30.

(f) R = 0.837; $\Delta\rho V/\overline{\rho V}$ = 0.30.

Figure 7. - Oscillograms showing propagating stall amplitude variation with radius for single-stage compressor with hub-tip ratio of 0.8. Compressor operating at point A of figure 4. f = 1120; $N/\sqrt{\theta}$ = 162; α = 60°; λ = 8.

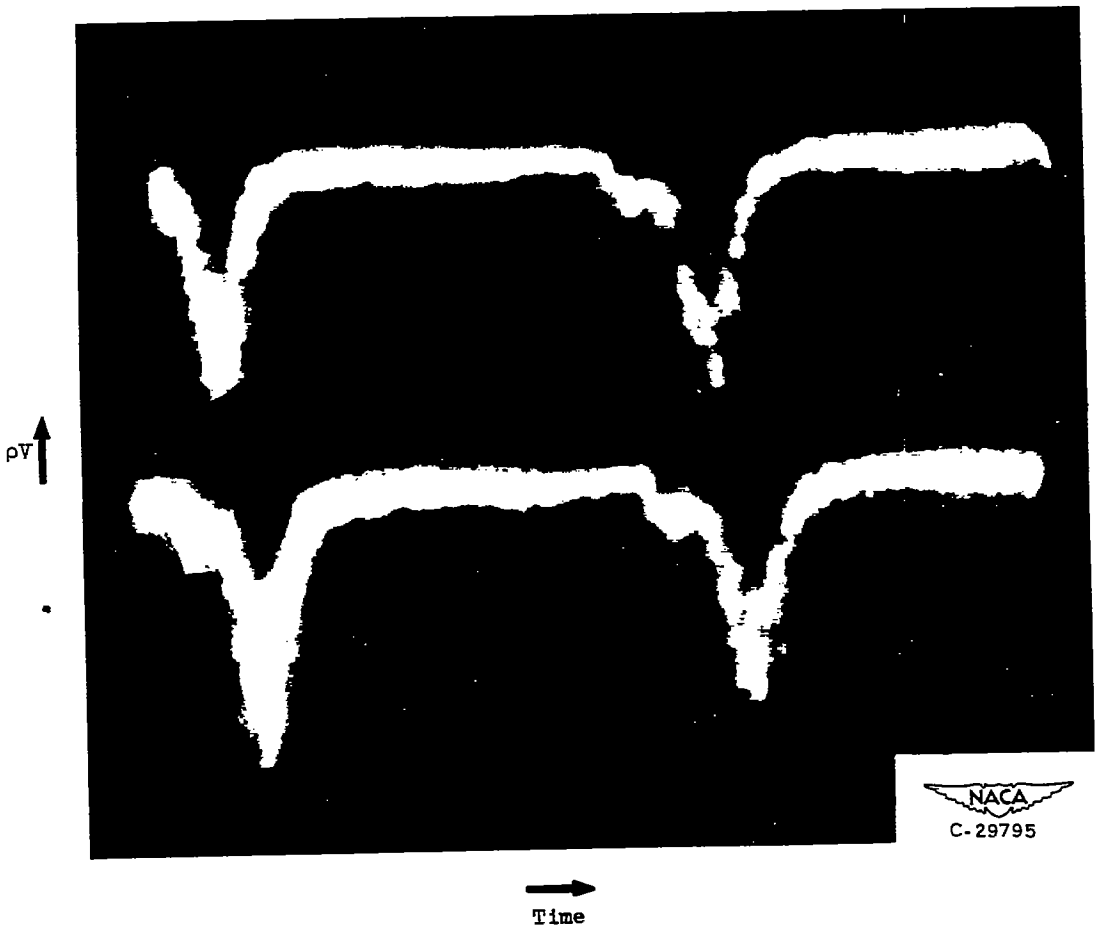

Figure 8. - Hot-wire anemometer oscillogram of propagating stall for single-stage compressor with hub-tip ratio of 0.8. Compressor operating at point C of figure 4. R = 0.937; f = 59; $N/\sqrt{\theta}$ = 162; α = 30°; λ = 1; $\Delta\rho V/\overline{\rho V}$ = 1.30.

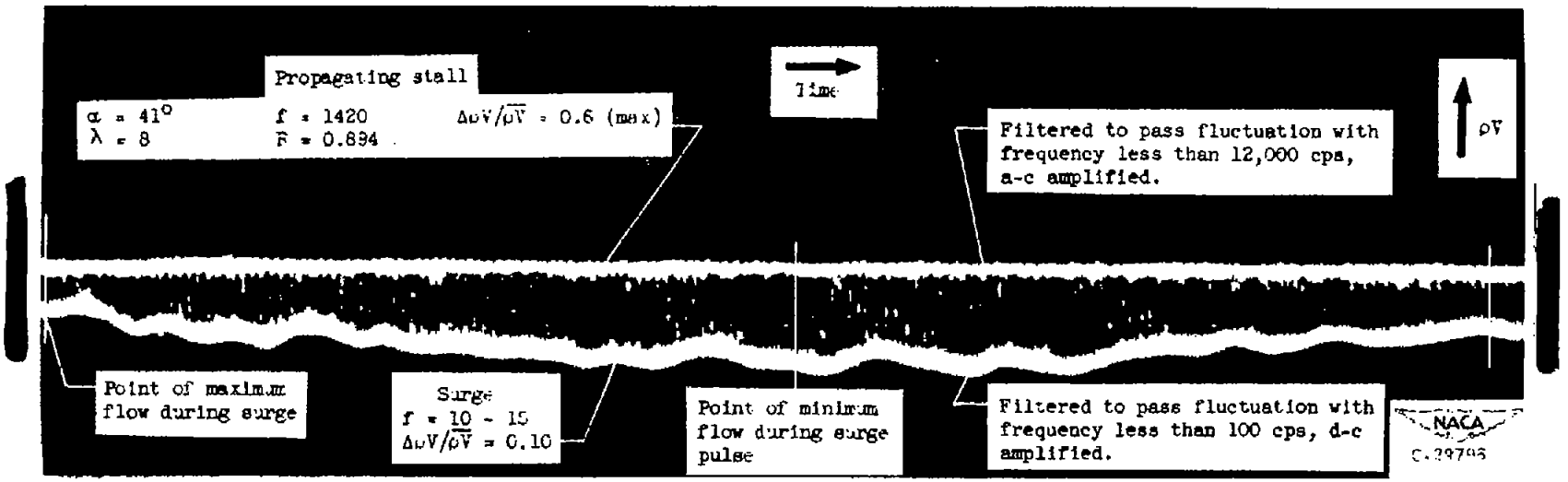

Figure 9. - Hot-wire anemometer oscillogram of flow fluctuations during surge for single-stage compressor with hub-tip ratio of 0.8. Compressor operating at point F of figure 4. $N/\sqrt{\theta} = 203$.

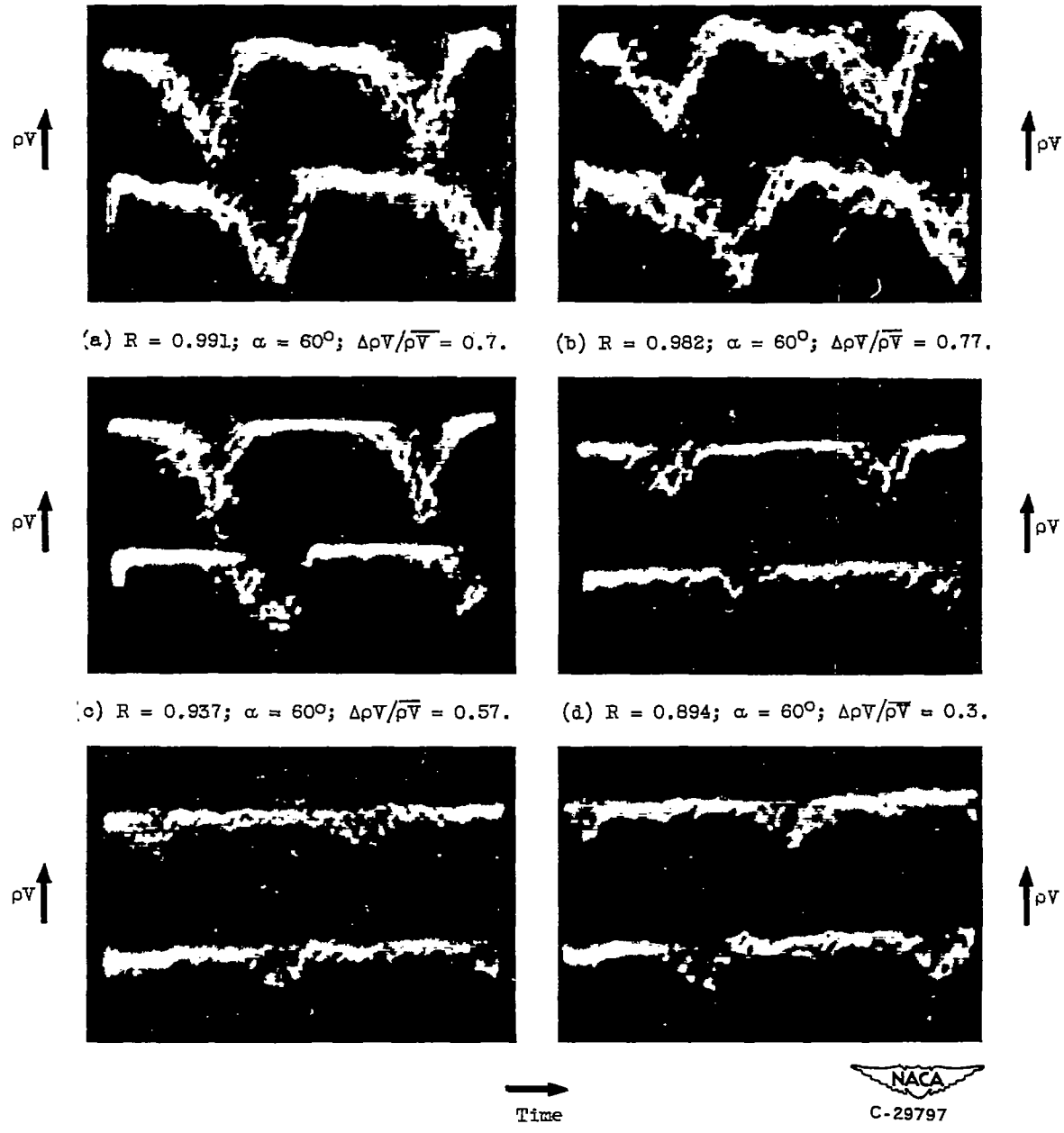

(a) R = 0.991; α = 60°; $\Delta\rho V/\overline{\rho V}$ = 0.7.

(b) R = 0.982; α = 60°; $\Delta\rho V/\overline{\rho V}$ = 0.77.

(c) R = 0.937; α = 60°; $\Delta\rho V/\overline{\rho V}$ = 0.57.

(d) R = 0.894; α = 60°; $\Delta\rho V/\overline{\rho V}$ = 0.3.

(e) R = 0.851; α = 30°; $\Delta\rho V/\overline{\rho V}$ = 0.2

(f) R = 0.837; α = 30°; $\Delta\rho V/\overline{\rho V}$ = 0.2.

Figure 10. - Hot-wire anemometer oscillogram of propagating stall for single-stage compressor with hub-tip ratio of 0.8. Compressor operating at point G of figure 5. f = 1420; $N/\sqrt{\theta}$ = 203; λ = 8.

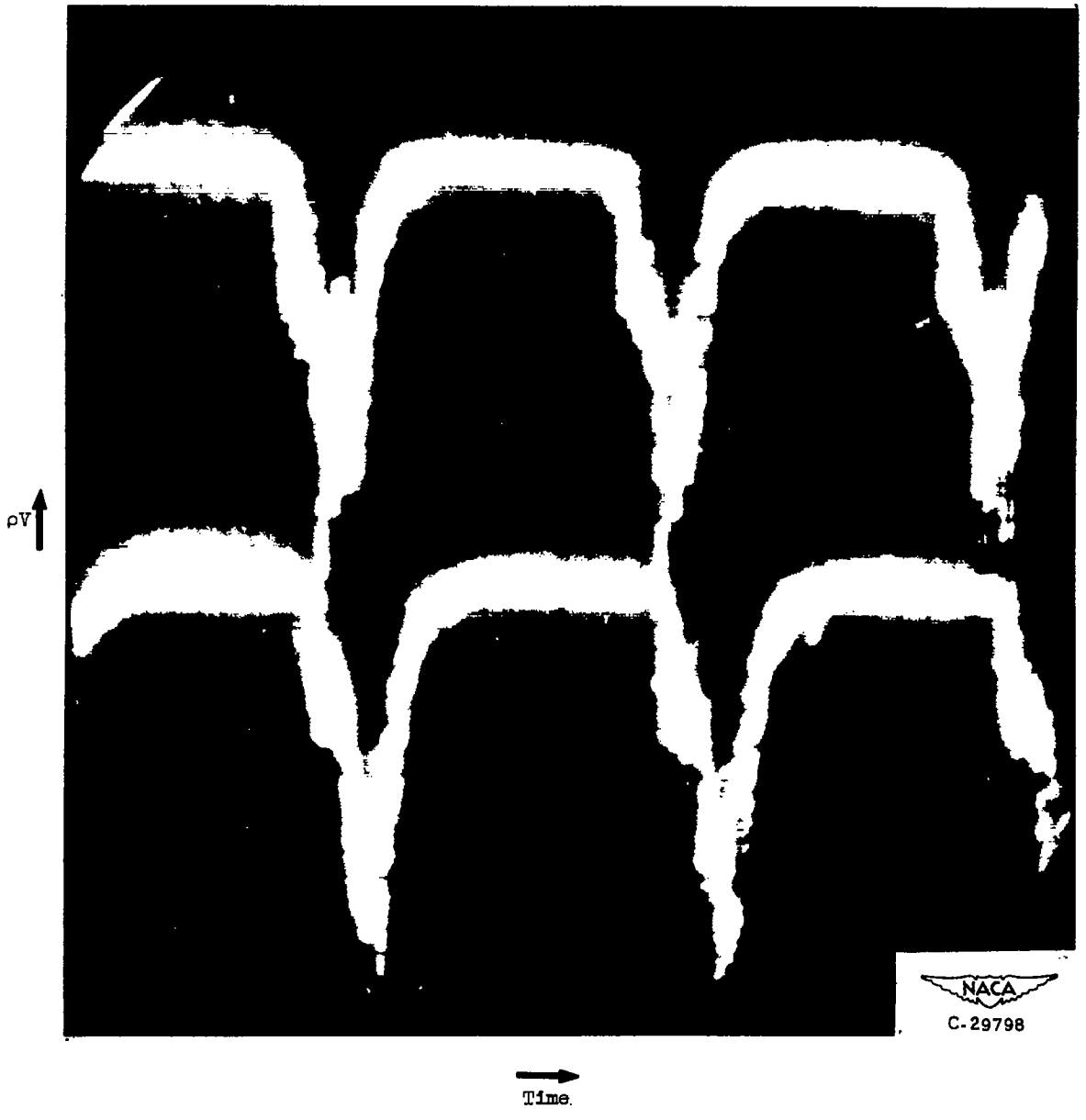

Figure 11. - Hot-wire anemometer oscillogram of rotating stall for single-stage compressor with hub-tip ratio of 0.8. $R = 0.937$; $f = 77$; $N/\sqrt{\theta} = 203$; $\alpha = 41\frac{1}{4}^{\circ}$; $\lambda = 1$; $\Delta\rho V/\overline{\rho V} = 1.2$. Compressor operating at point I of figure 5.

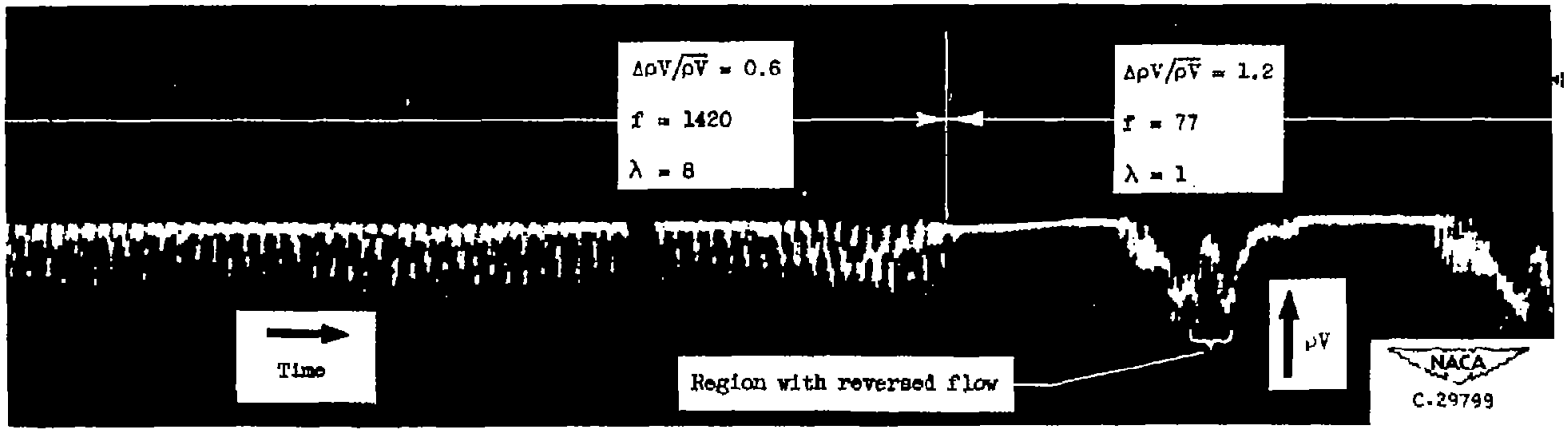

Figure 12. - Transition from eight rotating stalls at a frequency of 1420 cps to a single stall at a frequency of 77 cps as outlet throttle was closed for single-stage compressor with hub-tip ratio of 0.8. $N/\sqrt{\theta}$ = 203.

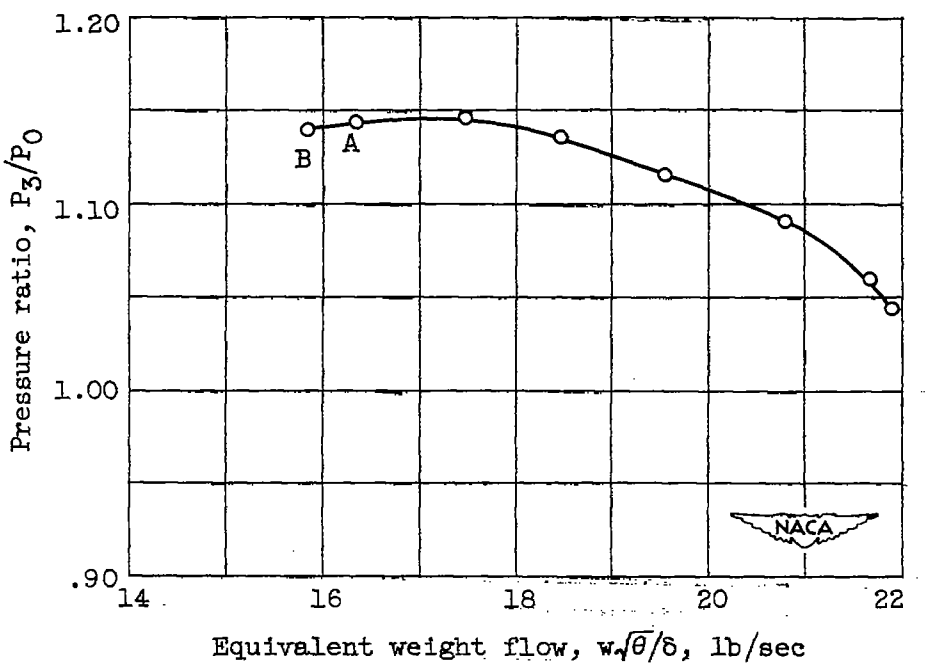

Figure 13. - Over-all performance of single-stage compressor with hub-tip ratio of 0.5. See figure 14 for radial surveys at position B. Initial tip stall is at position A. $N/\sqrt{\theta}$ = 225.

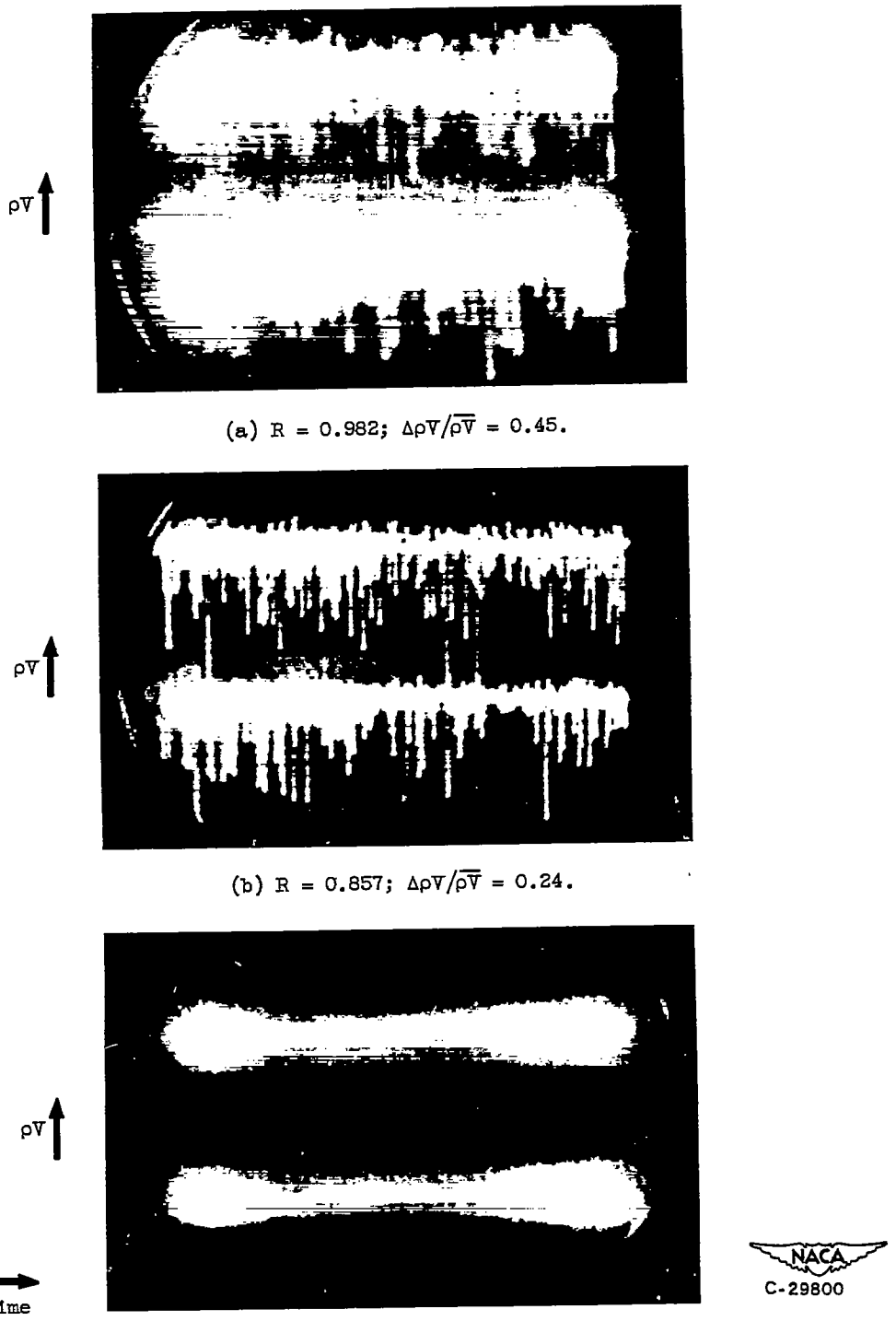

Figure 14. - Oscillograms showing propagating stall amplitude variation with radius for single-stage compressor with hub-tip ratio of 0.5. Compressor operating at point B of figure 13. f = 1200; $N/\sqrt{\theta}$ = 225.

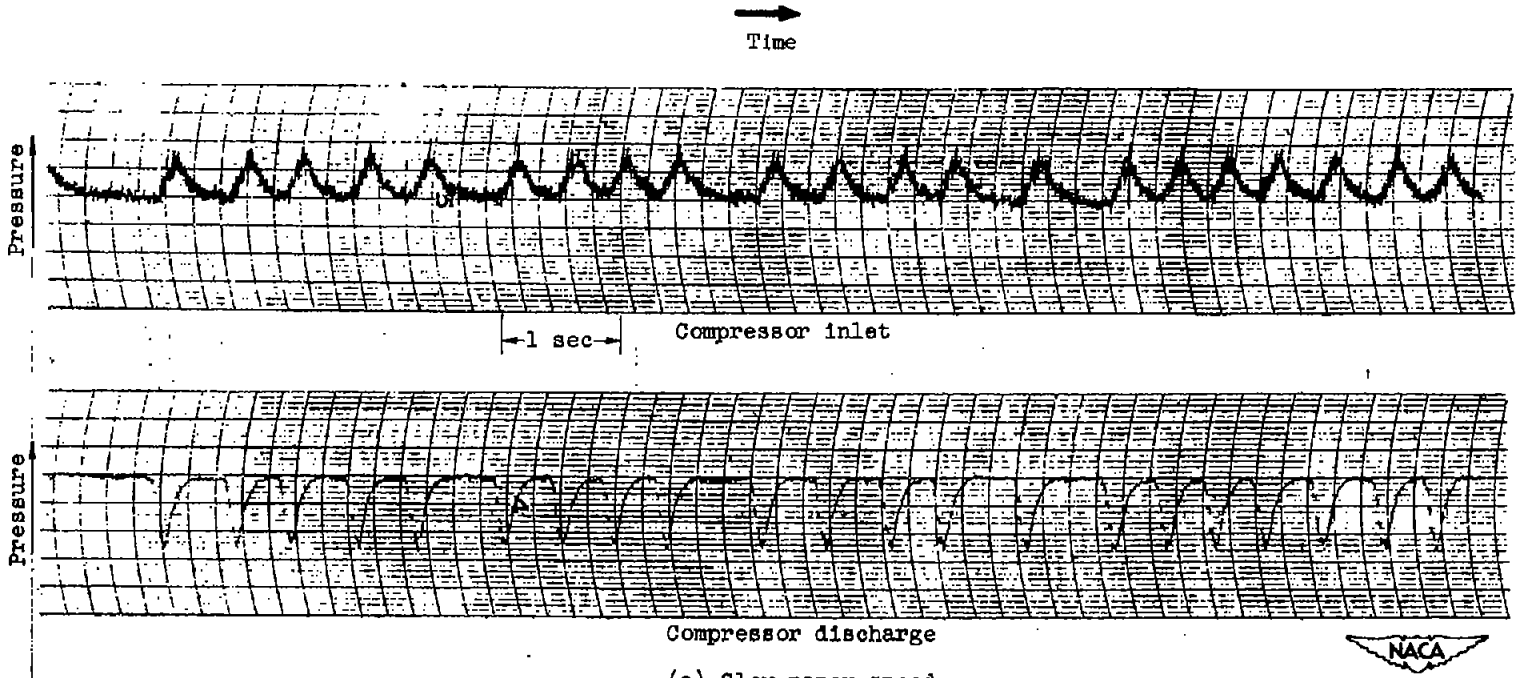

(a) Slow paper speed.

Figure 15. - Stagnation pressure variations at compressor inlet and discharge during surge for multistage compressor. $N/\sqrt{\theta} = 51$; large receiver volume; inlet $\Delta P/P_0 = +0.085$; discharge $\Delta P/P_3 = -0.17$.

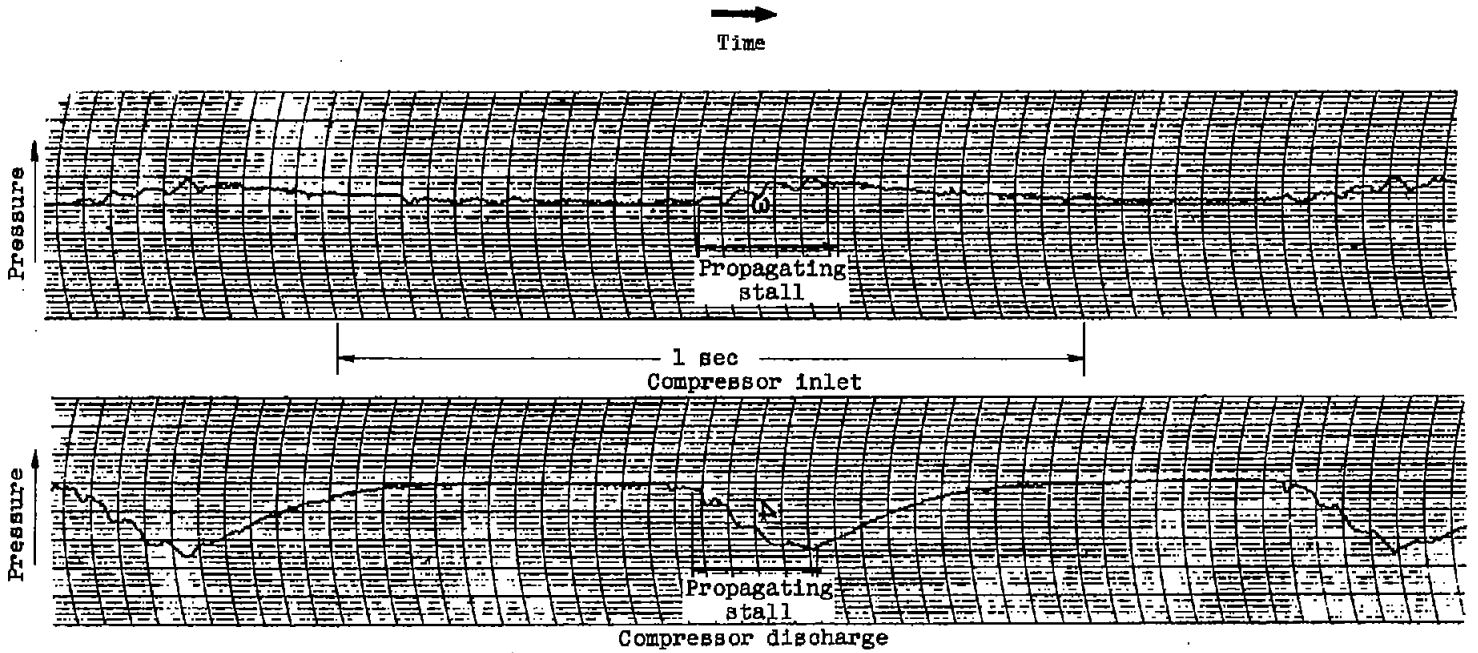

(b) High paper speed.

Figure 15. - Concluded. Stagnation pressure variations at compressor inlet and discharge during surge for multistage compressor. $N/\sqrt{\theta}$ = 51; large receiver volume; inlet $\Delta P/P_0$ = +0.085; discharge $\Delta P/P_3$ = -0.17.

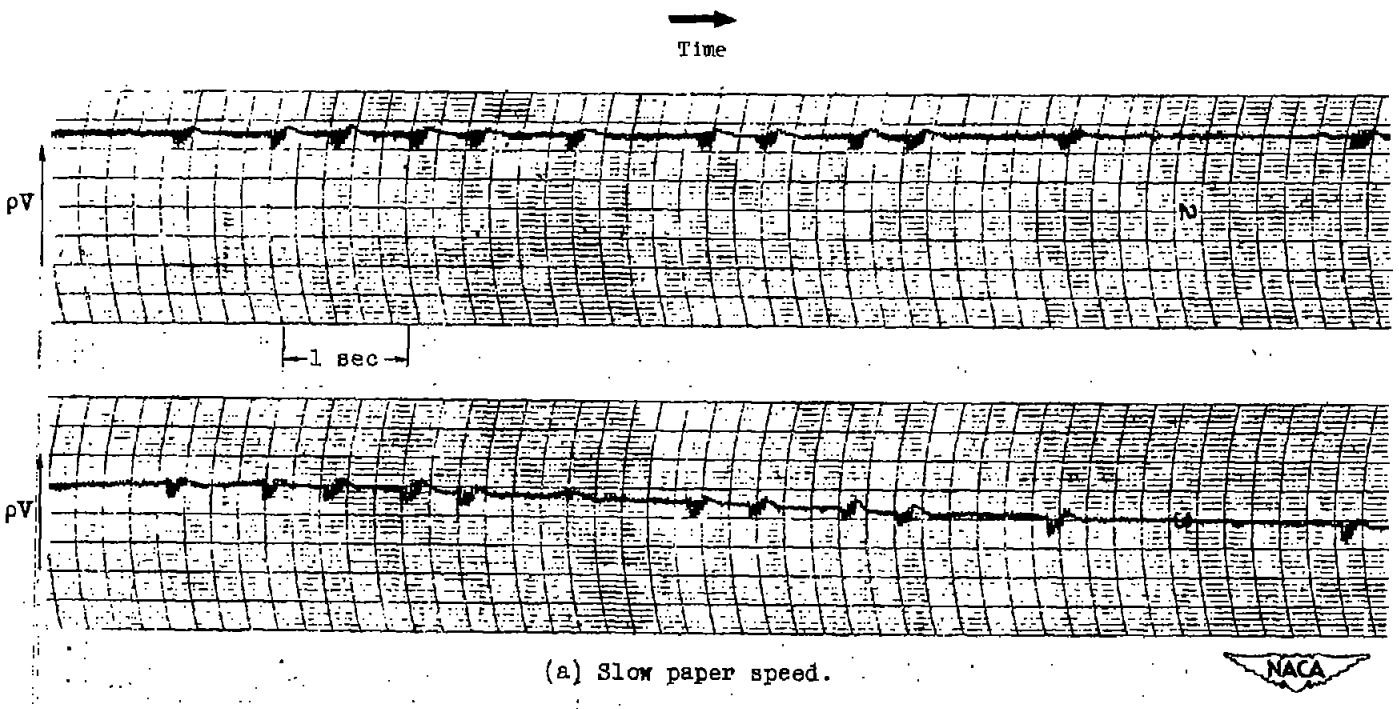

(a) Slow paper speed.

Figure 16. - Hot-wire anemometer output during surge; anemometer located in the seventh stage stator of multistage compressor. $N/\sqrt{\theta} = 51$; large receiver volume; $\alpha = 105^{\circ}$; surge $\Delta\rho V/\overline{\rho V} = \pm 0.3$; propagating stall $\Delta\rho V/\overline{\rho V} = 1.2$.

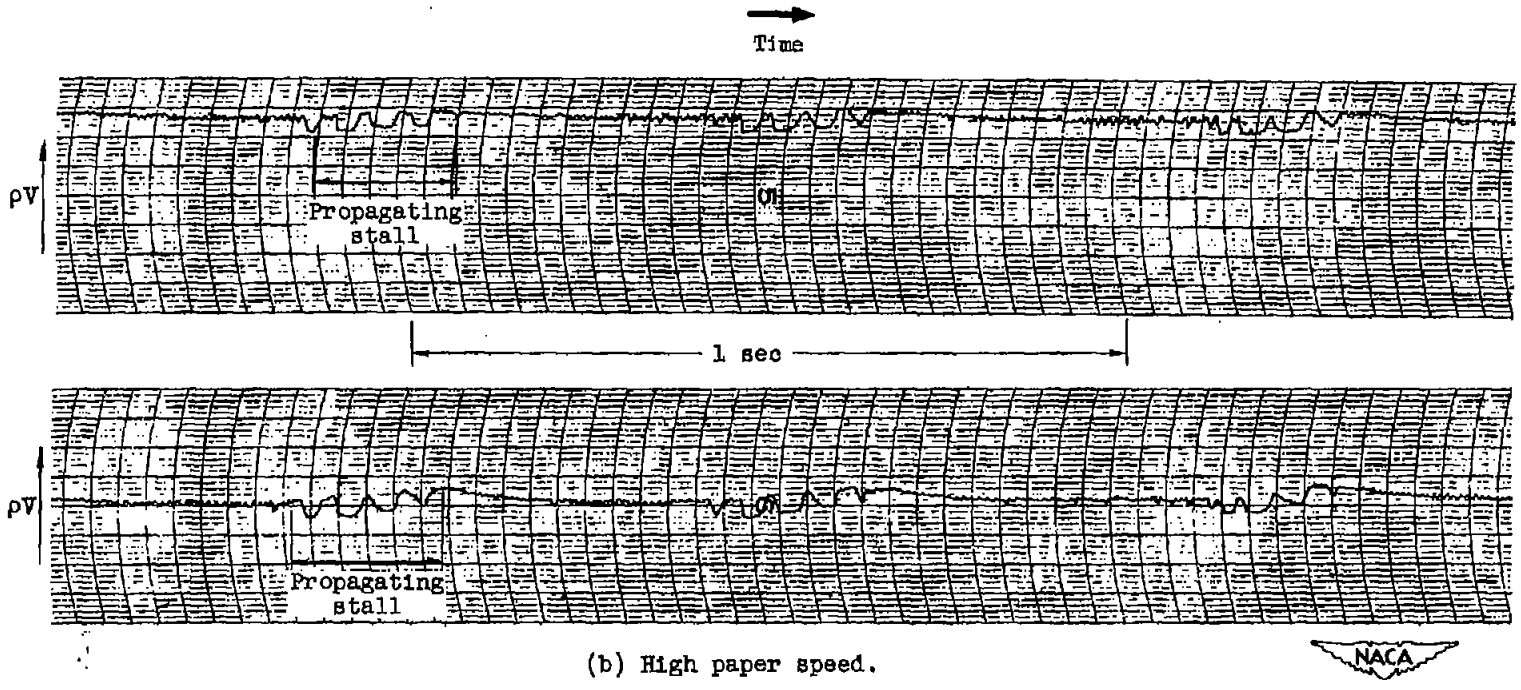

(b) High paper speed.

Figure 16. - Concluded. Hot-wire anemometer output during surge; anemometer located in the seventh stage stator of multistage compressor. $N/\sqrt{\theta} = 51$; large receiver volume; $\alpha = 105^{\circ}$; surge $\Delta\rho V/\overline{\rho V} = \pm 0.3$; propagating stall $\Delta\rho V/\overline{\rho V} = 1.2$.

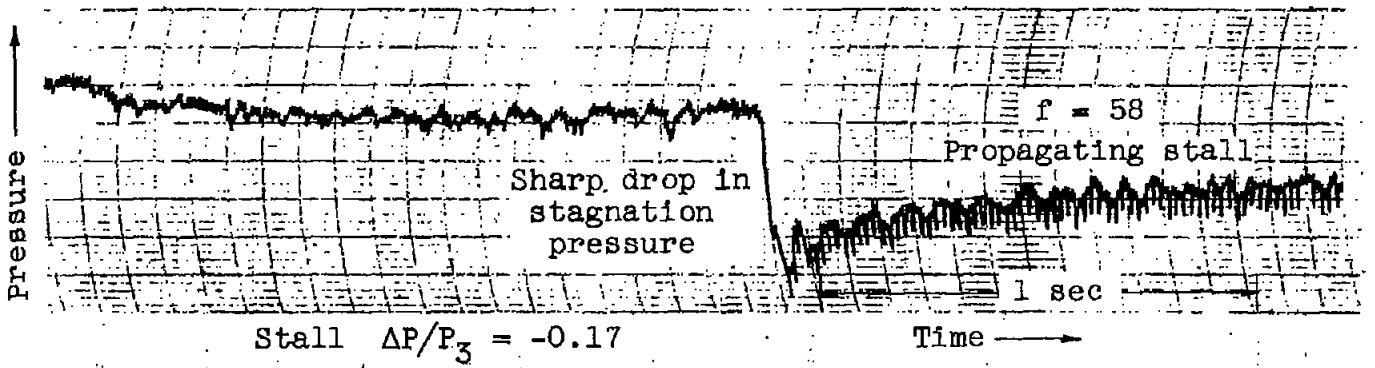

(a) Slow paper speed.

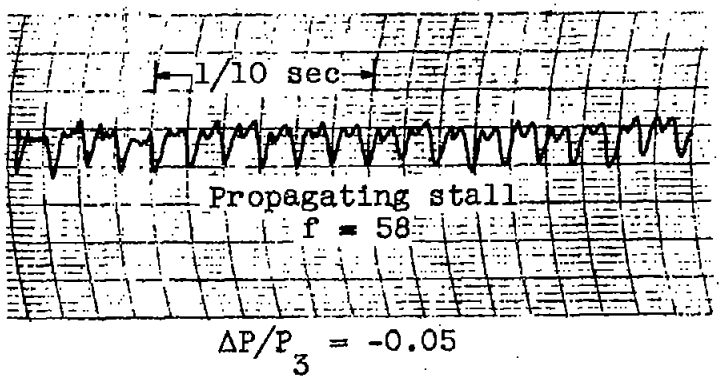

(b) High paper speed.

NACA

Figure 17. - Stagnation pressure variation at compressor discharge as surge line is crossed. Multistage compressor. $N/\sqrt{\theta}$ = 53; small receiver volume.

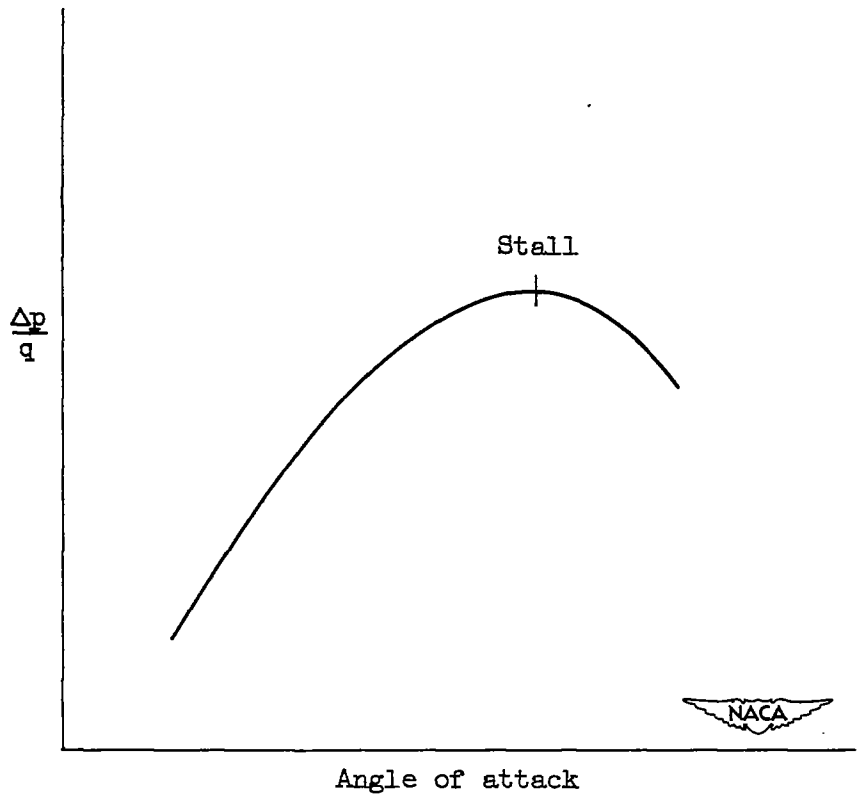

Figure 18. - Two-dimensional cascade stall characteristics.

[redacted]

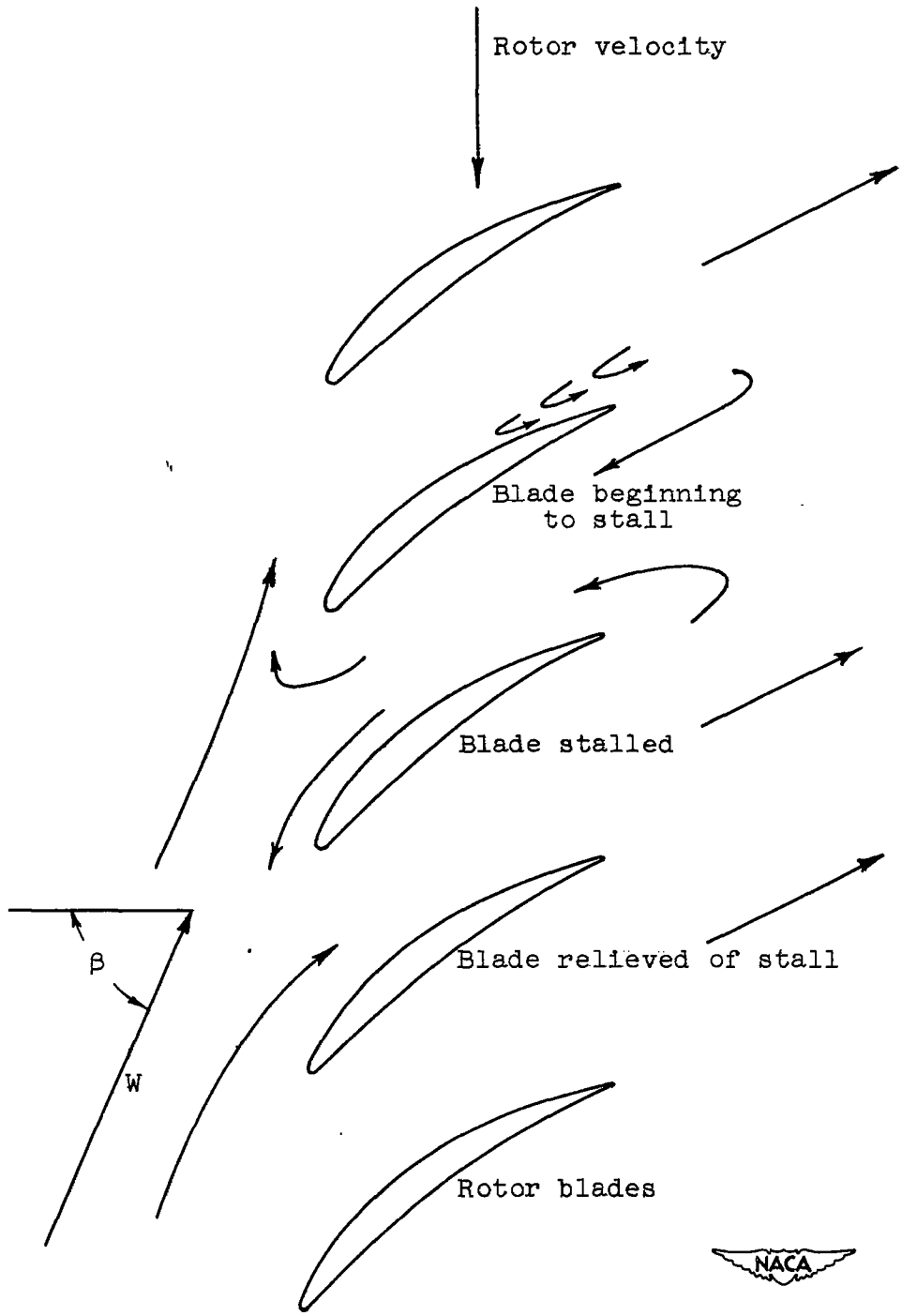

Figure 19. - Manner in which stall propagates from blade to blade.

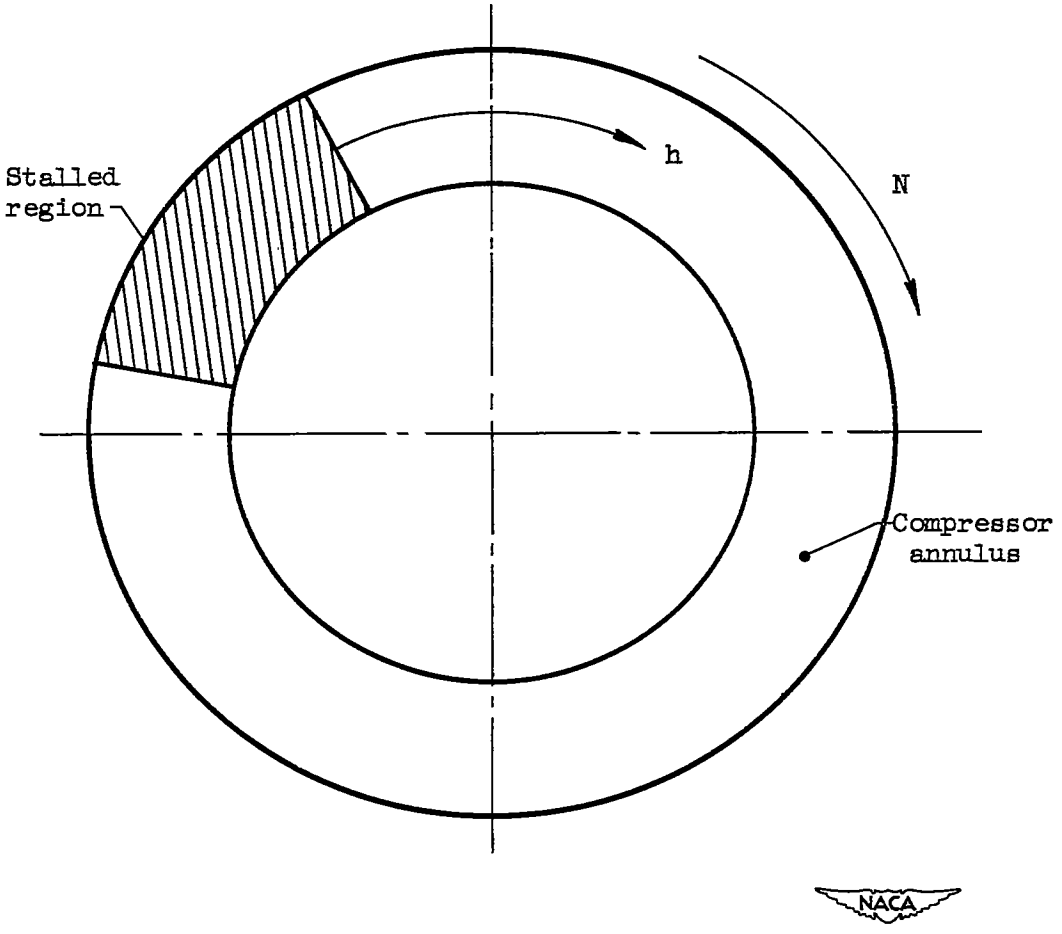

Figure 20. - Sketch indicating motion of propagating stall.

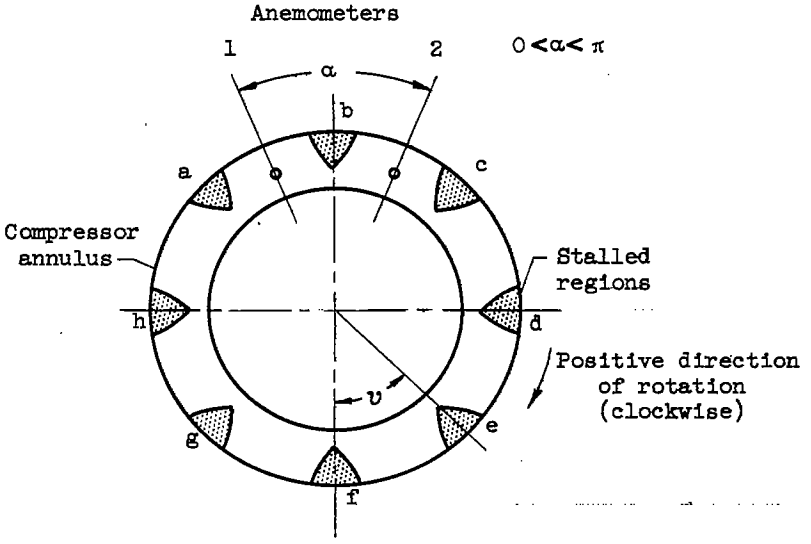

(a) Sketch showing anemometer location and propagating stall in compressor annulus.

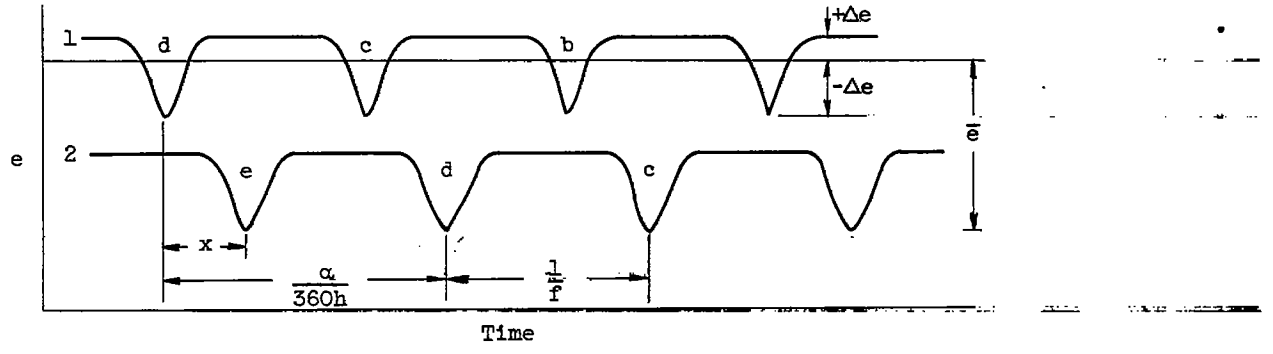

(b) Oscillogram from cathode ray oscilloscope, clockwise rotation of stall.

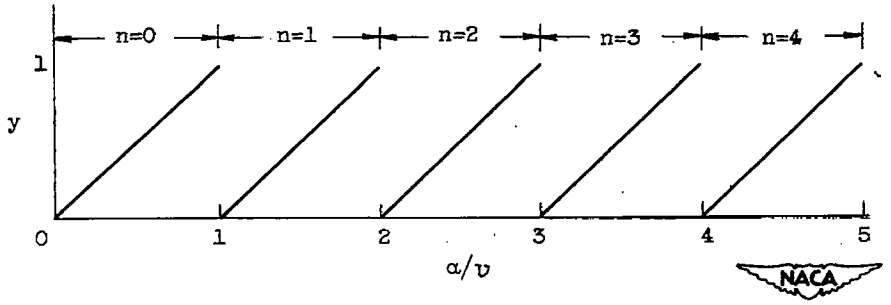

(c) Variation of y with α/v, clockwise rotation of stall.

Figure 21. - Relations necessary for determining number of propagating stalls.

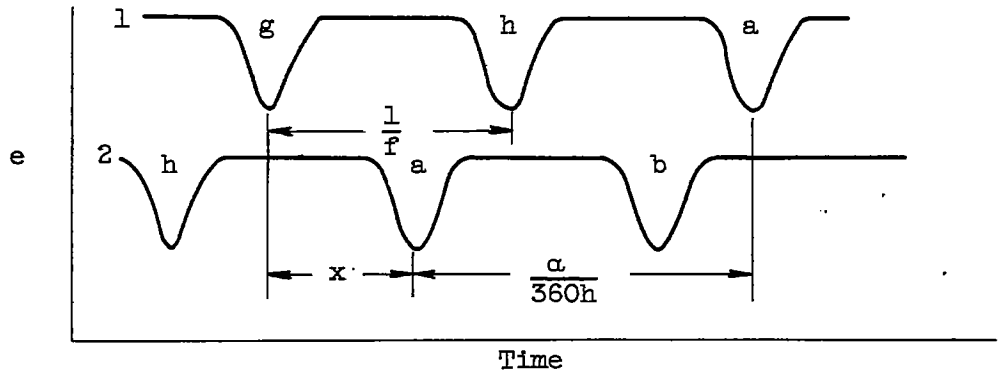

(d) Oscillogram from cathode ray oscilloscope, counterclockwise rotation of stall.

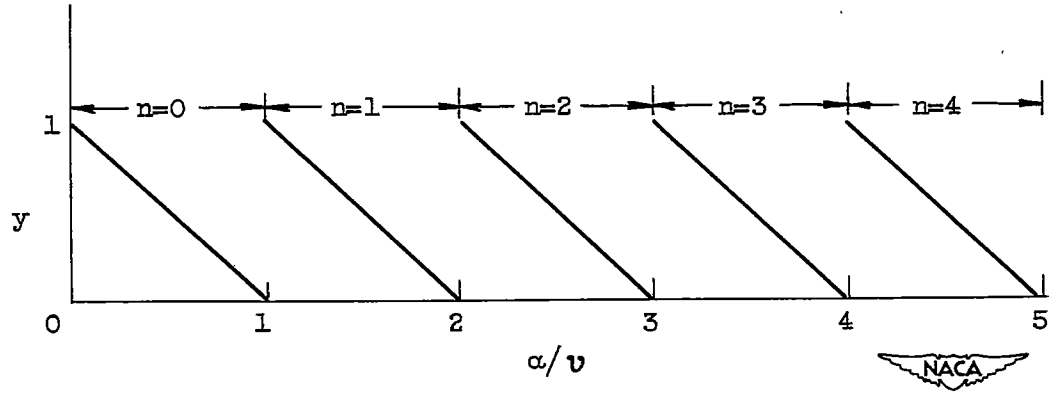

(e) Variation of y with α/v, counterclockwise rotation of stall.

Figure 21. - Concluded. Relations necessary for determining number of propagating stalls.

[redacted]

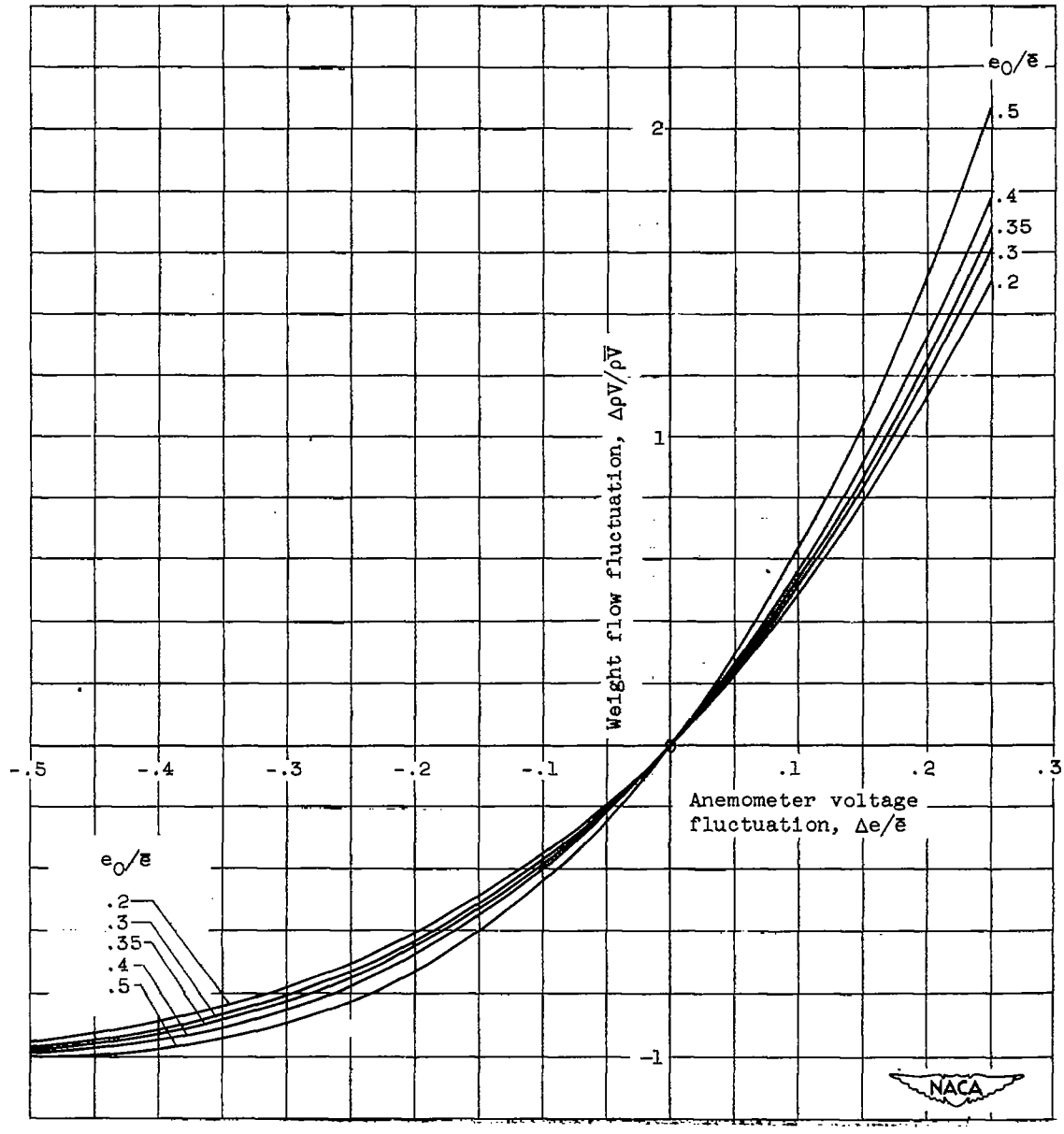

Figure 22. - Variation of weight flow fluctuations with anemometer voltage fluctuation.